

FILE COPY
NO 5

~~RESTRICTED~~

RM L51J05

NACA RM L51J05

THIS DOCUMENT ON LOAN FROM THE FILES OF



NATIONAL ADVISORY COMMITTEE FOR AERONAUTICS
LANGLEY AERONAUTICAL LABORATORY
LANGLEY FIELD, HAMPTON, VIRGINIA

RETURN TO THE ABOVE ADDRESS.

REQUESTS FOR PUBLICATIONS SHOULD BE ADDRESSED AS FOLLOWS:

RESEARCH MEMORANDUM

NATIONAL ADVISORY COMMITTEE FOR AERONAUTICS
12 F STREET, N.W.
WASHINGTON 25, D.C.

LOW-SPEED INVESTIGATION OF THE EFFECTS OF WING LEADING-
EDGE MODIFICATIONS AND SEVERAL OUTBOARD FIN
ARRANGEMENTS ON THE STATIC STABILITY
CHARACTERISTICS OF A LARGE-SCALE
TRIANGULAR WING

By H. Clyde McLemore

Langley Aeronautical Laboratory
Langley Field, Va.

CLASSIFICATION CANCELLED	
Authority <u>Crowley</u>	Date <u>12-11-53</u>
By <u>T. C. F.</u>	Release form no. <u>1826</u>

NATIONAL ADVISORY COMMITTEE FOR AERONAUTICS

WASHINGTON
January 10, 1952

~~RESTRICTED~~

NATIONAL ADVISORY COMMITTEE FOR AERONAUTICS

RESEARCH MEMORANDUM

LOW-SPEED INVESTIGATION OF THE EFFECTS OF WING LEADING-
EDGE MODIFICATIONS AND SEVERAL OUTBOARD FIN

ARRANGEMENTS ON THE STATIC STABILITY

CHARACTERISTICS OF A LARGE-SCALE

TRIANGULAR WING

By H. Clyde McLemore

SUMMARY

An investigation of a large-scale triangular wing having 60° of leading-edge sweep and with 10-percent-thick circular-arc airfoil sections parallel to the plane of symmetry was made in the Langley full-scale tunnel to determine the effects of wing leading-edge modifications and several outboard fin arrangements on the low-speed static stability characteristics.

The results of the present investigation indicate that rounding the wing leading edge by installing a nose glove having ordinates corresponding to the NACA 65(06)-006.5 airfoil delayed the vortex flow and alleviated the accompanying force and moment breaks characteristic of the wing with sharp leading edges. A further increase of the wing leading-edge radius by installing an NACA 65-010 nose glove eliminated the force and moment breaks associated with vortex flow.

Installing outboard fins in several spanwise and chordwise locations on the wings indicated that the most desirable over-all stability characteristics were obtained with the fins located as far outboard as practical and with the leading edge of the fin tangent to the leading-edge profile of the wing. Fins placed in the most effective location increased the lift coefficient at which negative dihedral was experienced and also produced the best directional stability characteristics.

Increasing the Reynolds number from approximately 2.7×10^6 to approximately 9.7×10^6 produced only a minor influence on the static stability characteristics of the three configurations investigated with

fins removed or installed. The large-scale data obtained for the present investigation are in reasonable agreement with the low-scale data obtained previously.

INTRODUCTION

Previous investigations of the pressure distribution and force characteristics of triangular wings (references 1 to 4) have shown the existence of leading-edge separation and an accompanying strong vortex flow for wings having sharp leading edges or small leading-edge radii. From such information available in reference 3, it was known that modifying the wing leading edge by changing the nose radii would alleviate the leading-edge separation and vortex flow and the accompanying force and moment breaks. It has also been shown that this vortex flow becomes weaker as the wing leading-edge radius is increased (reference 3). The flow investigation reported in reference 2 shows that the separation vortices increase in size and intensity as they progressively sweep inboard and away from the wing leading edge with increasing angle of attack. The progression of this type of flow over the wing surface would be expected to influence considerably the stability characteristics as have been indicated in low-scale tests (reference 5) and the characteristics of a control surface installed in its path (reference 6).

The present tests were conducted in the Langley full-scale tunnel to determine the effects of wing leading-edge modifications and several outboard fin arrangements on the low-speed static stability characteristics of a large-scale triangular wing having 10-percent-thick circular-arc airfoil sections.

The wing leading-edge modifications investigated were nose gloves having airfoil ordinates corresponding to the NACA 65₍₀₆₎-006.5 and NACA 65-010 airfoil sections with leading-edge radii of 0.282 percent chord and 0.687 percent chord, respectively. The effects of the fins were investigated at three chordwise positions at the 45-percent-semispan station, two chordwise positions at the 60-percent-semispan station, and one chordwise position at the 75-percent-semispan station.

The tests were conducted through a Reynolds number range from 2.90×10^6 to 9.72×10^6 with a greater portion of the tests conducted at a Reynolds number of 6.00×10^6 corresponding to a Mach number of 0.07.

SYMBOLS

The test data are presented as standard NACA coefficients of forces and moments referred to the stability axes as indicated in figure 1. The origin of the system of axes is located in the plane of symmetry of the wing at a point projected from the quarter chord of the mean aerodynamic chord.

C_L	lift coefficient (L/qS)
$C_{L_{max}}$	maximum lift coefficient
C_X	longitudinal-force coefficient (X/qS)
C_m	pitching-moment coefficient ($M/qS\bar{c}$)
C_Y	lateral-force coefficient (Y/qS)
C_l	rolling-moment coefficient (L'/qSb)
C_n	yawing-moment coefficient (N/qSb)
L	total lift of wing ($-Z$)
Z	vertical force
X	longitudinal force
D	total drag of wing ($-X$)
Y	lateral force
L/D	lift-to-drag ratio
M	pitching moment about Y-axis
L'	rolling moment about X-axis
N	yawing moment about Z-axis
q	free-stream dynamic pressure ($\rho V^2/2$)
ρ	mass density of air
V	free-stream velocity

S	wing area
R	Reynolds number
Λ	angle of sweepback at wing leading edge, degrees
\bar{c}	mean aerodynamic chord measured parallel to plane of symmetry $\left(\frac{2}{S} \int_0^{b/2} c^2 dy \right)$
y	spanwise coordinate
c	local chord
b	wing span
α	angle of attack measured in plane of symmetry, degrees
ψ	angle of yaw (positive when right semispan is rearward), degrees
A	aspect ratio
λ	taper ratio
$C_{l\psi}$	rate of change of rolling-moment coefficient with angle of yaw, per degree
$C_{n\psi}$	rate of change of yawing-moment coefficient with angle of yaw, per degree
$C_{Y\psi}$	rate of change of lateral-force coefficient with angle of yaw, per degree

Subscripts:

t	upper surface
b	lower surface
w	wing
f	fins

MODEL

The wing used in this investigation was triangular in plan form with the leading edge sweptback 60° , and had circular-arc airfoil sections parallel to the plane of symmetry with a maximum thickness of 10 percent of the chord located at 50 percent of the chord. The wing had an aspect ratio of 2.31, a span of 23.1 feet, and an area of 231 square feet. Geometric characteristics of the basic wing (hereafter referred to as configuration A) are given in figure 2. A photograph of the wing mounted for tests in the Langley full-scale tunnel is given as figure 3. The wing had no geometric dihedral or twist and was constructed entirely of metal.

The leading-edge modifications investigated were gloves having airfoil ordinates corresponding to NACA 65(06)-006.5 and NACA 65-010 airfoil sections (fig. 4) and will be referred to as configurations B and C, respectively, throughout the remainder of the paper. The ordinates for the gloves are given in table I. The gloves for configurations B and C are faired into the basic wing at the 25- and 50-percent-chord lines, respectively. The juncture of the glove with the wing surface was made smooth and fair by the use of modeling clay.

Two types of fins were investigated, and the geometric characteristics of the fins and their arrangements on the wing are shown in figure 5. Fin 1 had a leading-edge sweepback angle of 53° and was mounted on the upper surface of the wing, and fin 2 had a leading-edge sweepback angle of 45° and was installed in two parts, one on the upper and one on the lower surface of the wing. Fins 1 and 2 had an aspect ratio of 1.4 and were constructed of $\frac{3}{4}$ -inch plywood rigidly supported by cables attached to the wing surface. The fins can be located at three chordwise stations at $0.45\frac{b}{2}$, two chordwise stations at $0.60\frac{b}{2}$, and one chordwise station at $0.75\frac{b}{2}$. (See fig. 5.)

Fin 2 was not tested on configuration C because the lower portion of fin 2 could not be supported by the sheet metal forming the glove.

TESTS

In order to determine the static longitudinal and lateral stability characteristics of the wing, force tests were made at zero yaw for angles of attack from 0° through the stall and for yaw angles of

approximately $\pm 2^\circ$, $\pm 4^\circ$, 8° , 10° , and 16° for angles of attack from 0° to just below the stall.

The effects of the three leading-edge contours on the longitudinal aerodynamic characteristics both with fins removed and installed were investigated at Reynolds numbers of 2.90×10^6 , 6.00×10^6 , and 9.72×10^6 with corresponding Mach numbers of 0.02, 0.07, and 0.12. The tests in yaw were made at a Reynolds number of 6.00×10^6 . The flow over the fins was investigated by observing the action of wool tufts attached to the fins in position 45-3 (fig. 5) for all wing leading-edge configurations.

RESULTS AND DISCUSSION

Presentation of Results

The results of the present paper have been corrected for stream misalignment, bouyancy, and the effects of blocking and jet boundary. Support strut tares were not applied for it was determined in reference 1 that these effects on the present wing are negligible.

The results of the tests are grouped into two main sections. The first section presents the static longitudinal stability characteristics of the three wing configurations with outboard fins removed and installed and includes figures 6 to 12. Curves are presented in figure 7 showing the results of tests of each of the wing configurations with the fins located in the position that resulted in the most desirable static longitudinal stability characteristics. The second section presents the static lateral stability characteristics of the three wing configurations with outboard fins removed and installed and includes figures 13 to 19. Summary curves showing the lateral-stability parameters C_{L_ψ} , C_{n_ψ} , and C_{Y_ψ} for the configurations with fins installed in the various positions investigated are given in figure 13. Summary curves of the lateral-stability parameters for the configurations with fins removed and installed in the most effective position are given in figure 14.

Static Longitudinal Stability Characteristics

Effect of wing leading-edge modifications.- The variations of angle of attack, longitudinal-force and pitching-moment coefficients with lift coefficient for the three wing configurations investigated with outboard fins removed are given in figure 6. Configuration A had the characteristic vortex-type flow reported in references 1 and 2 for wings having

10-percent-thick circular-arc airfoil sections and triangular plan forms. The existence of the vortex flow was indicated in the present investigation by the force and moment breaks that occur at lift coefficients of 0.4 to 0.6. It has been shown that a bubble of separation, characteristic of airfoils having sharp or small-radius leading edges, forms along the leading edge at low angles of attack, and develops into a conical-separation vortex which increases in strength and size and gradually moves inboard as angle of attack is increased. The effect of the vortex on the chordwise loading as shown in reference 2 was to reduce the leading-edge pressures but at the same time broaden the region of high chordwise loading with the result that the section lift-curve slope was increased as long as there was reattachment of the flow behind the bubble of separation. When there was no reattachment of the flow behind the bubble of separation, the section was stalled. The complete separation and accompanying abrupt loss in lift occurred over the outer portion of the wing at an angle of attack of about 14° , corresponding to a lift coefficient of approximately 0.6. (See fig. 6.) The sudden loss in lift of the outer portion of wing A resulted in a rapid forward shift of center of pressure with a decrease of longitudinal stability. A more complete discussion of the effects of the vortex-type flow over triangular and related pointed-tip wings is given in reference 2.

Rounding the wing leading edge to a radius of approximately 0.0028c by the installation of a nose glove having airfoil ordinates corresponding to the NACA 65₍₀₆₎-006.5 airfoil section (configuration B) improved the longitudinal stability characteristics. The slope of the lift curve in the low-to-moderate lift-coefficient range was lower than that for configuration A and the increase in lift-curve slope due to the vortex flow was less and occurred at a slightly higher lift coefficient. This was due probably to a delay in the formation of the vortex. The longitudinal stability of configuration B as indicated by the variation of C_m with C_L was about the same as that for configuration A in the low-lift-coefficient range, but for lift coefficients of about 0.2 to 0.5 the longitudinal stability was increased. Except for a trim shift, the longitudinal stability above a lift coefficient of about 0.6 was approximately the same as for configuration A. The longitudinal-force coefficients were slightly lower for a given lift coefficient through the moderate lift-coefficient range than those obtained for configuration A.

Further increase of the wing leading-edge radius to approximately 0.0069c by installing a nose glove having airfoil ordinates corresponding to the NACA 65-010 airfoil section (configuration C) appeared to eliminate completely the effects of vortex-type flow. The lift, longitudinal-force, and pitching-moment curves through the complete lift-coefficient range did not exhibit the abrupt changes noted for configurations A and B. The wing was longitudinally stable through the lift-coefficient range and the stability increased with increasing lift coefficients through most

of the lift-coefficient range with a slight decrease in stability occurring at a lift coefficient of about 1.0. The longitudinal-force coefficient was lower for a given lift coefficient than for either configurations A or B.

It was found in reference 3 that rounding the wing leading edge to a radius larger than $0.0025c$ had small effects on the static longitudinal stability characteristics, but it is felt this small effect was due to the very thin wing sections ($0.045c$) used on the wing investigated.

Effect of fins and fin position.- The results of installing outboard fins at several spanwise and chordwise locations on configurations A, B, and C for Reynolds numbers varying from about 2.9×10^6 to 9.7×10^6 are given in figures 7 to 12. An increase in Reynolds number from approximately 2.9×10^6 to 6.0×10^6 had a small but inconsistent effect on the static longitudinal stability characteristics of the three wings; therefore, the following discussion will be for an average Reynolds number of approximately 6×10^6 .

The results of the fin tests indicate that the most desirable location of the fins from the standpoint of the longitudinal stability characteristics will be outboard as far as practical and with the leading edge tangent to the wing profile near the wing leading edge. Moving the fins away from the wing leading edge caused abrupt force and moment breaks. Similar results were obtained at low scale on a triangular wing having NACA 65₍₀₆₎-006.5 airfoil sections and are reported in reference 5. Comparison of these data with reference 5 indicate that large-scale outboard fin effects can be reasonably estimated by low-scale investigations.

The results of installing outboard fins in position 75-1 on the three wing configurations investigated are given in figure 7. It will be noted that the fin installations reduced $C_{L_{max}}$ by approximately 0.15. A reduction in $C_{L_{max}}$ was noted for all other fin positions (see figs. 8 to 12) and seems to be a characteristic of outboard-located fins (references 5 and 7). Maximum lift as indicated by the peak of the lift curve, however, may not have significance for the triangular wing at approach or landing speeds because of the very high angle of attack ($\alpha \approx 35^\circ$) required to reach this lift coefficient. For a more practical angle-of-attack range (20° or less), the installation of fins in position 75-1 had little effect on the lift coefficient. The installation of fins in position 75-1 had negligible effects on the variations of the pitching-moment coefficients with lift coefficient. The longitudinal-force coefficients for the angle-of-attack range increased slightly for a given lift coefficient for lift coefficients greater than 0.4 for configurations A and B when the fins were installed in position 75-1; however, the

longitudinal-force coefficients for configuration C were slightly decreased, for lift coefficients from 0.4 to 0.7.

The values of L/D for configurations A, B, and C for a lift-coefficient range of 0.4 to 0.8 with fins removed and installed in position 75-1 are given in figure 7(b). The installation of fins in position 75-1 produces only minor changes in the values of L/D for the lift-coefficient range presented.

The effects of fin 1 on the lift, longitudinal-force, and pitching-moment coefficients of configuration A are given in figure 8. Fin 1 placed tangent to the wing profile at the leading edge at any of the spanwise positions gave more favorable force and moment characteristics than did the more rearward fin positions. With the fins placed at the wing leading edge, the separation vortex that normally extends outboard along the wing leading edge (reference 2) was turned downstream upon contact with the fins; thereby preventing the high tip loading associated with the vortex flow. The result was a relatively smooth variation of the lift curve through the usable angle-of-attack range. There was, however a slight range of neutral stability with the fins in position 75-1 at a lift coefficient of about 0.4, and this was probably due to stalling of the portion of the wing outboard of the fins. With the fins placed in the other spanwise positions investigated (rearward from the wing leading edge) the vortex was allowed to form and progress along the wing surface in the manner previously discussed until it swept back far enough to contact the fins. There it was directed downstream, inboard of the fins, with the result that the wing area outboard of the fins stalled, causing abrupt force and moment breaks. (See fig. 8(b).) It will be noted that the force and moment breaks occurred at higher angles of attack as the fins were placed in positions further removed from the wing leading edge. In order to verify the discussion on the flow characteristics about outboard, vertical fins installed on the subject wing, flow tests were made on a 6-foot span, 60° delta-wing model mounted in the Langley full-scale tunnel. Fins were installed on the model in positions corresponding to positions 60-1, 45-1, and 45-2. The flow tests were made by visually observing the action of a long wool surface probe and wool tufts attached to the wing surface. The type of flow observed was in agreement with the discussion in the present paper.

Replacing fin 1 by fin 2 produced negligible changes in the force and moment characteristics. (See fig. 9.) The maximum-lift coefficient was slightly increased when fin 2 was installed.

The effects of fin 1 on the lift, longitudinal-force, and pitching-moment coefficients of configuration B are shown in figure 10. Fin position 45-2 was omitted from this series of tests as an undesirable position. Fin position 45-1 was omitted from the tests because of attachment difficulties caused by the nose glove installation. The same

order of fin effect was noted on configuration B as was noted for configuration A. Fin position 75-1 was the most desirable position investigated for this configuration, and again position 45-3 (the position farthest removed from the wing leading edge) produced the most adverse effects on the stability characteristics.

Replacing fin 1 by fin 2 (fig. 11) again produced negligible changes on the force and moment characteristics. Fin position 60-2 was omitted from the fin 2 tests as an undesirable position.

The results of installing fin 1 on configuration C are given in figure 12. It was previously noted that wing leading-edge modifications eliminated the effects of vortex flow over configuration C with fins removed. For this configuration with fins installed, the force and moment breaks were probably due to stalling of the area outboard of the fins. It was also noted that the outboard side of the fins in position 45-3 were stalled for lift coefficients at which the force and moment breaks occurred. For the fin positions investigated, position 75-1 provided the smoothest variations of the force and moment curves throughout the lift-coefficient range. It will be noted that all the force and moment breaks occurred at an angle of attack of 20° or greater.

All the configurations investigated, either with fins removed or installed, were longitudinally stable near and through $C_{L_{max}}$; however, the destabilizing tendencies in the low-to-moderate lift-coefficient range represent trim shifts which may not be manageable.

Static Lateral Stability Characteristics

The static-lateral-stability parameters C_{l_ψ} , C_{n_ψ} , and C_{y_ψ} , presented as a function of lift coefficient in figures 13 and 14, were determined by measuring the slopes of average linear curves faired through $\pm 4^\circ$ yaw from the data of figures 15 to 19.

Effect of wing leading-edge modifications.- The data of figure 13 (fins off) indicates that wing leading-edge modifications had little effect on the lateral stability characteristics. The greater wing leading-edge radii of configuration C produced a more nearly linear variation of C_{l_ψ} with C_L to a lift coefficient of about 0.5 than did configuration A; however, the maximum value of the effective dihedral parameter was about 0.002 at a lift coefficient of approximately 0.5 for the three configurations investigated. At a lift coefficient slightly above 0.5 the effective dihedral decreases rapidly for configurations A and B indicating that the leading semispan has stalled and the trailing semispan is maintaining lift due to the existence of the vortex flow. The effect of yaw on the flow pattern was determined by pressure measurements and flow studies made on a small-scale triangular wing having the same geometric characteristics as configuration A of the present paper and

reported in detail in reference 2. The effective dihedral for configuration C decreased rapidly above a lift coefficient of about 0.7 and became negative at a lift coefficient of about 0.8, whereas the effective dihedral for configurations A and B became negative at a lift coefficient of about 0.7. The loss in effective dihedral for configuration C at lift coefficients from 0.7 to 0.8 was similar to that for configurations A and B having sharper leading edges.

In general, the wing configurations with fins removed were directionally stable through the lift-coefficient range to a lift coefficient of about 0.9. The directional stability for configuration C was slightly greater than for configurations A and B, and the lift coefficient where instability occurred was increased to approximately 1.0.

The data of figure 13 (fins off) shows that the values of $C_{Y\psi}$ in the low-lift-coefficient range were essentially zero for the three wing configurations investigated. For lift coefficients greater than approximately 0.7 the values of $C_{Y\psi}$ increased rapidly with increasing lift coefficient. This rapid increase in the values of $C_{Y\psi}$ was again probably due to the flow breakdown over the leading semispan.

Effect of fins and fin position.- The variations of the static lateral stability characteristics with lift coefficient for the three wing configurations investigated with fins removed or installed in the various positions noted in figure 4 are given in figure 13. It is shown in figure 13 that all the fin positions that located the leading edge of the fins tangent to the profile of the wing at the leading edge produced desirable lateral stability characteristics. As the fins were moved farther inboard and behind the wing leading edge the lateral stability became increasingly adverse. In general, the effective dihedral parameter $C_{L\psi}$ had a maximum value of approximately 0.002 at lift coefficients of about 0.6 to 0.7 for the three wing configurations investigated with fins installed in the various positions. The wings were directionally stable throughout the lift-coefficient range investigated with fins installed in any of the positions. (See fig. 13.)

The variations of $C_{L\psi}$, $C_{n\psi}$, and $C_{Y\psi}$ with C_L for the three wing configurations investigated with fins installed in position 75-1 are given in figure 14. Fin position 75-1 was selected because its effects on the lateral stability characteristics of the three wing configurations were slightly more favorable than the other positions investigated (fig. 13), and also because it was one of the most effective positions indicated previously in the discussion of the static longitudinal stability characteristics. This position was also found to be the most effective position in the static low-scale investigation given in reference 5.

As shown in figure 14 the installation of fins in position 75-1 on the three wing configurations investigated increased slightly the lift coefficient at which the effective dihedral becomes negative. Fin 2 installed in this position produced lower values of effective dihedral throughout the lift-coefficient range than those produced by fin 1. The directional stability for fin 1 in this position, however, was greater (and essentially constant at a value of approx. -0.004) than that for fin 2; and, therefore, fin 1 was considered more desirable. The effective dihedral for configuration C with fin 1 installed remained positive throughout the lift-coefficient range; however, sharp breaks occurred at lift coefficients of about 0.7 to 0.8 corresponding to the lift coefficients where the force and moment breaks occurred in the longitudinal stability characteristics. A loss in directional stability was experienced above a lift coefficient of approximately 0.7 for the configurations with fin 1 installed in position 75-1; however, directional stability was maintained to the stall.

SUMMARY OF RESULTS

The results of an investigation in the Langley full-scale tunnel to determine the effects of wing leading-edge modifications and several outboard fin arrangements on the low-speed static longitudinal and lateral stability characteristics of a large-scale triangular wing having 10-percent-thick circular-arc airfoil sections and 60° of leading-edge sweep are summarized as follows:

1. Rounding the wing leading edge to a radius of approximately 0.0028c by installing a nose glove having ordinates corresponding to the NACA 65(06)-006.5 airfoil delayed the vortex flow and alleviated the accompanying force and moment breaks characteristic of the wing with sharp leading edges. Further increase of the wing leading-edge radius to a value of approximately 0.0069c by installing an NACA 65-010 nose glove eliminated force and moment breaks associated with vortex flow.

2. Increasing the Reynolds number from approximately 2.7×10^6 to approximately 9.7×10^6 produced minor effects on the static stability characteristics of the three configurations investigated with fins removed or installed, and the data obtained for the present investigation are in agreement with the low-scale data obtained previously.

3. The most desirable over-all stability characteristics were obtained with the fins located as far outboard as practical and with the fin leading edge tangent to the wing profile at the leading edge. With fins installed in the most outboard position, the lift coefficient at which negative effective dihedral was experienced was increased.

4. All the fins investigated provided directional stability through most of the lift-coefficient range. The most desirable directional stability characteristics were obtained with fin 1 located at 75 percent span and tangent to the wing leading edge profile.

Langley Aeronautical Laboratory
National Advisory Committee for Aeronautics
Langley Field, Va.

REFERENCES

1. Whittle, Edward F., Jr., and Lovell, J. Calvin.: Full-Scale Investigation of an Equilateral Triangular Wing Having 10-Percent-Thick Biconvex Airfoil Sections. NACA RM L8G05, 1948.
2. May, Ralph W., Jr., and Hawes, John G.: Low-Speed Pressure-Distribution and Flow Investigation for a Large Pitch and Yaw Range of Three Low-Aspect-Ratio Pointed Wings Having Leading Edge Swept Back 60° and Biconvex Sections. NACA RM L9J07, 1949.
3. Anderson, Adrien E.: An Investigation at Low Speed of a Large-Scale Triangular Wing of Aspect Ratio Two. II. The Effect of Airfoil Section Modifications and the Determination of the Wake Downwash. NACA RM A7H28, 1947.
4. Anderson, Adrien E.: Chordwise and Spanwise Loadings Measured at Low Speed on Large Triangular Wings. NACA RM A9B17, 1949.
5. Jaquet, Byron M., and Brewer, Jack D.: Effects of Various Outboard and Central Fins on Low-Speed Static-Stability and Rolling Characteristics of a Triangular-Wing Model. NACA RM L9E18, 1949.
6. Hawes, John G., and May, Ralph W., Jr.: Investigation at Low Speed of the Effectiveness and Hinge Moments of a Constant-Chord Ailavator on a Large-Scale Triangular Wing with Section Modification. NACA RM L51A26, 1951.
7. Goodman, Alex: Effect of Various Outboard and Central Fins on Low-Speed Yawing Stability Derivatives of a 60° Delta-Wing Model. NACA RM L50E12a, 1950.

TABLE I.- AIRFOIL ORDINATES PARALLEL TO PLANE OF

SYMMETRY OF WING CONFIGURATIONS TESTED

	Configuration A	Configuration B	Configuration C
Station (percent c)	Basic wing (10-percent circular arc)	Wing with NACA 65(06)-006.5 glove	Wing with NACA 65-010 glove
	Ordinates (\pm percent c)	Ordinates (\pm percent c)	Ordinates (\pm percent c)
0	----	----	----
.50	----	0.51	0.77
.75	----	.61	.93
1.25	0.25	.77	1.17
2.5	.49	1.03	1.57
5.0	.96	1.42	2.18
7.5	1.40	1.74	2.65
10	1.81	2.05	3.04
15	2.56	2.65	3.66
20	3.21	3.22	4.07
25	3.75	3.75	4.42
30	4.21	4.21	4.67
35	4.55	4.55	4.81
40	4.80	4.80	4.92
45	4.95	4.95	4.98
50	5.00	5.00	5.00
55	4.95	4.95	4.95
60	4.80	4.80	4.80
65	4.55	4.55	4.55
70	4.21	4.21	4.21
75	3.75	3.75	3.75
80	3.21	3.21	3.21
85	2.56	2.56	2.56
90	1.81	1.81	1.81
95	.96	.96	.96
100	----	----	----
		L.E. radius = 0.00282c	L.E. radius = 0.00687c

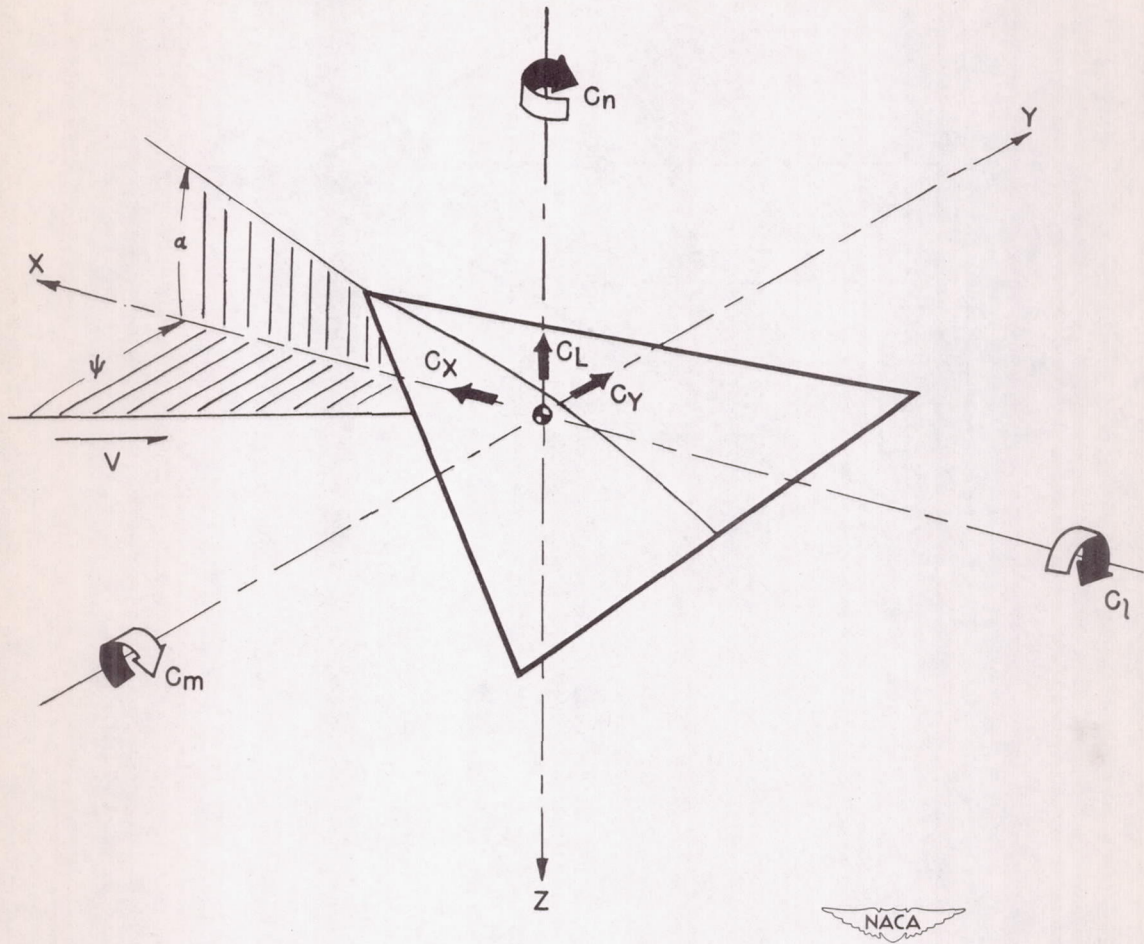
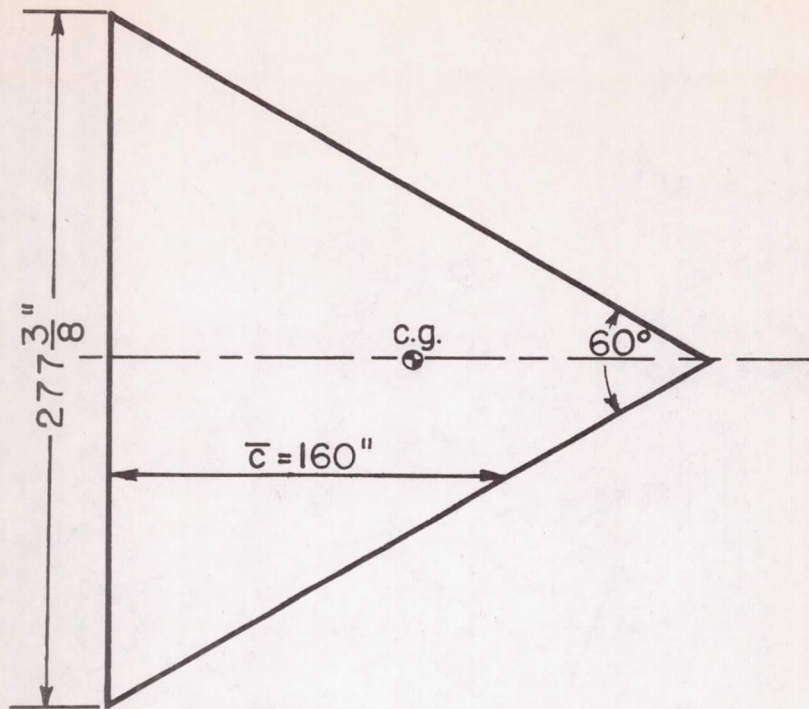


Figure 1.- The stability system of axes and sign convention for the standard NACA coefficients. All forces, force coefficients, moment coefficients, and angles are shown as positive.



Aspect Ratio 2.31
Area 231 sq ft.

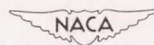
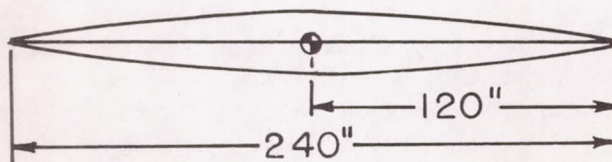


Figure 2.- Geometric characteristics of the wing without nose gloves installed. All dimensions are given in inches. Configuration A.

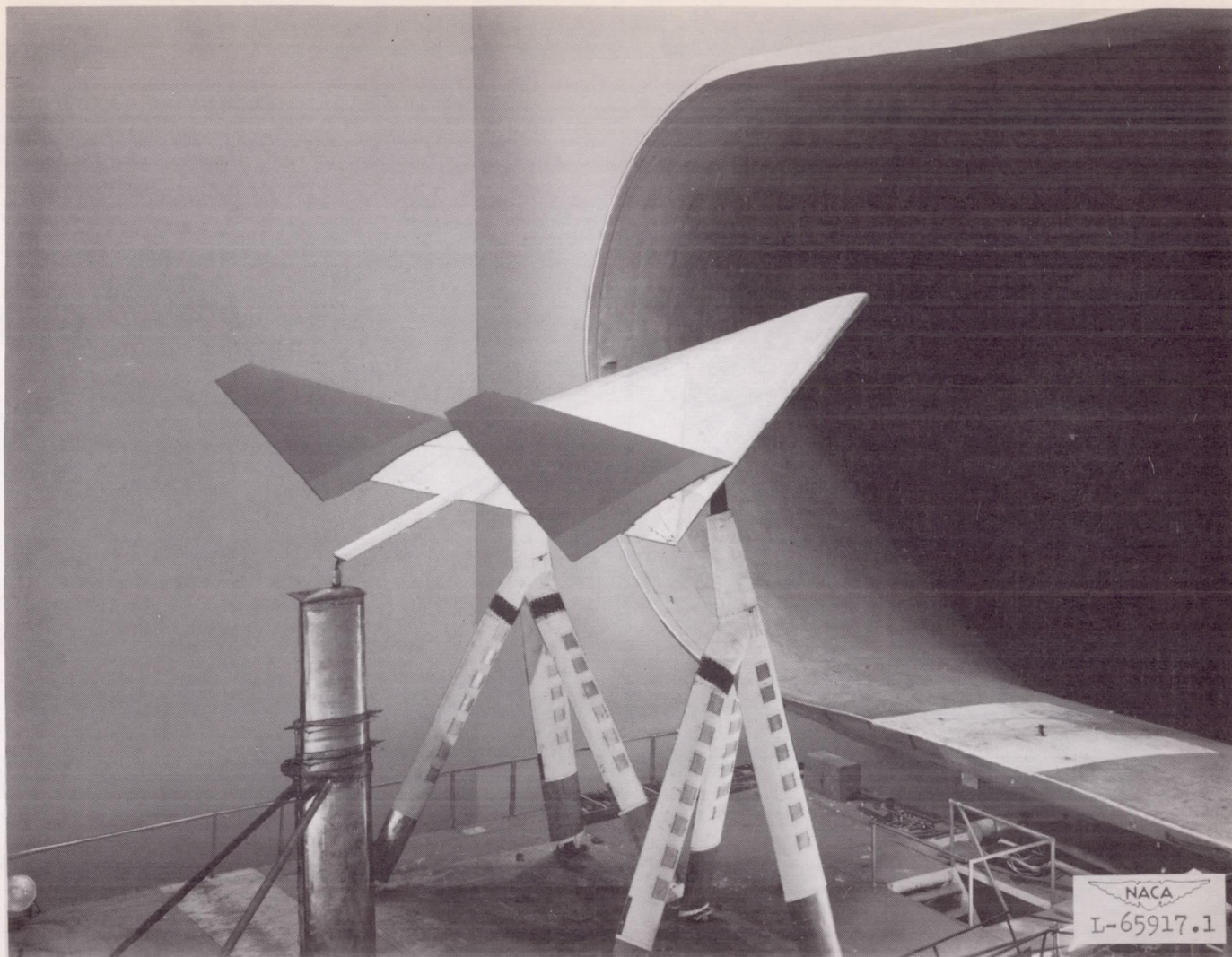
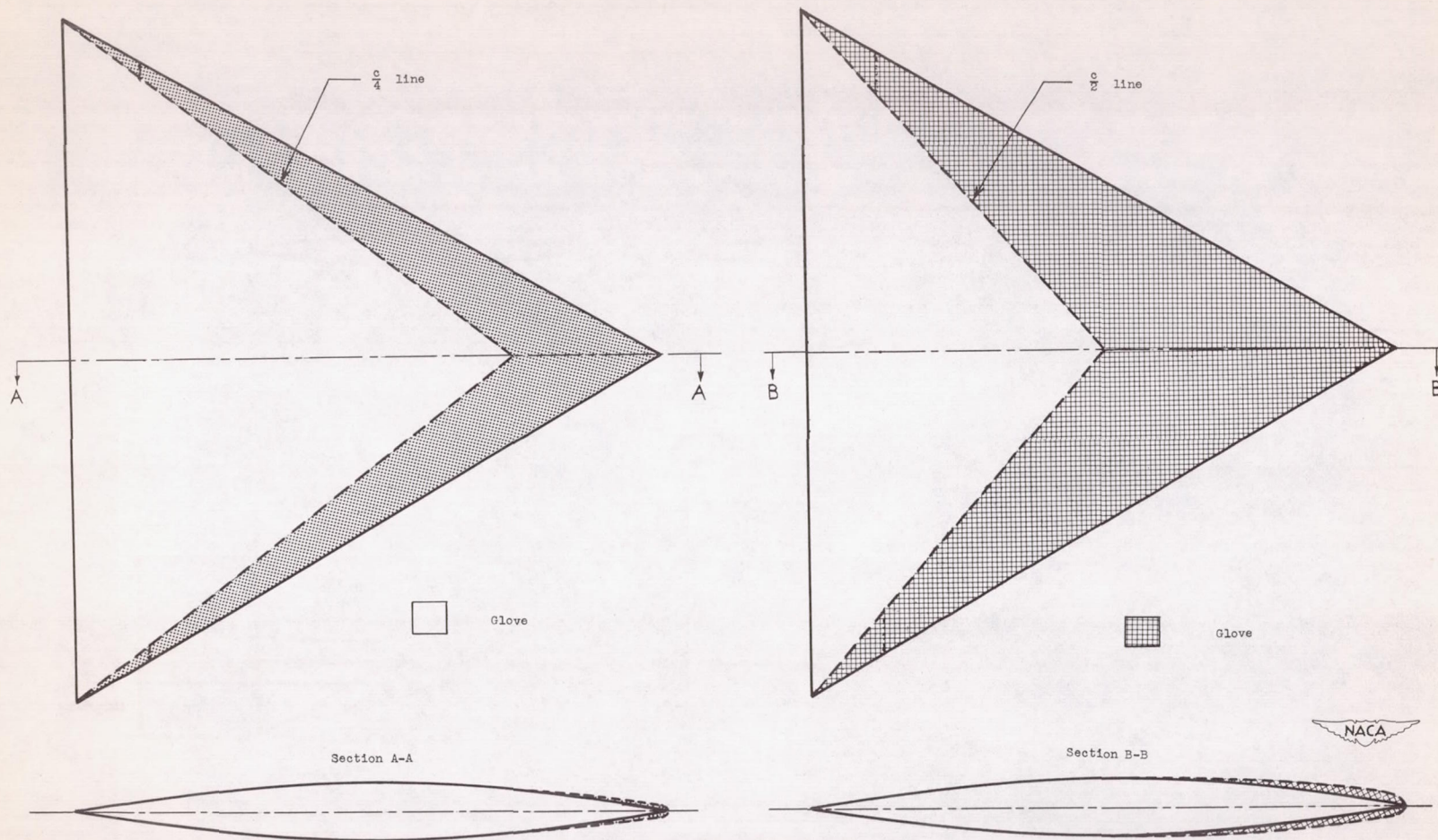


Figure 3.- Photograph of the wing mounted for tests in the Langley full-scale tunnel. Configuration C; fin 1; position 75-1.



(a) Wing with NACA 65(06)-006.5 nose glove. Configuration B. (b) Wing with NACA 65-010 nose glove. Configuration C.

Figure 4.- Geometric characteristics of nose gloves investigated. Airfoil ordinates are given in table 1.

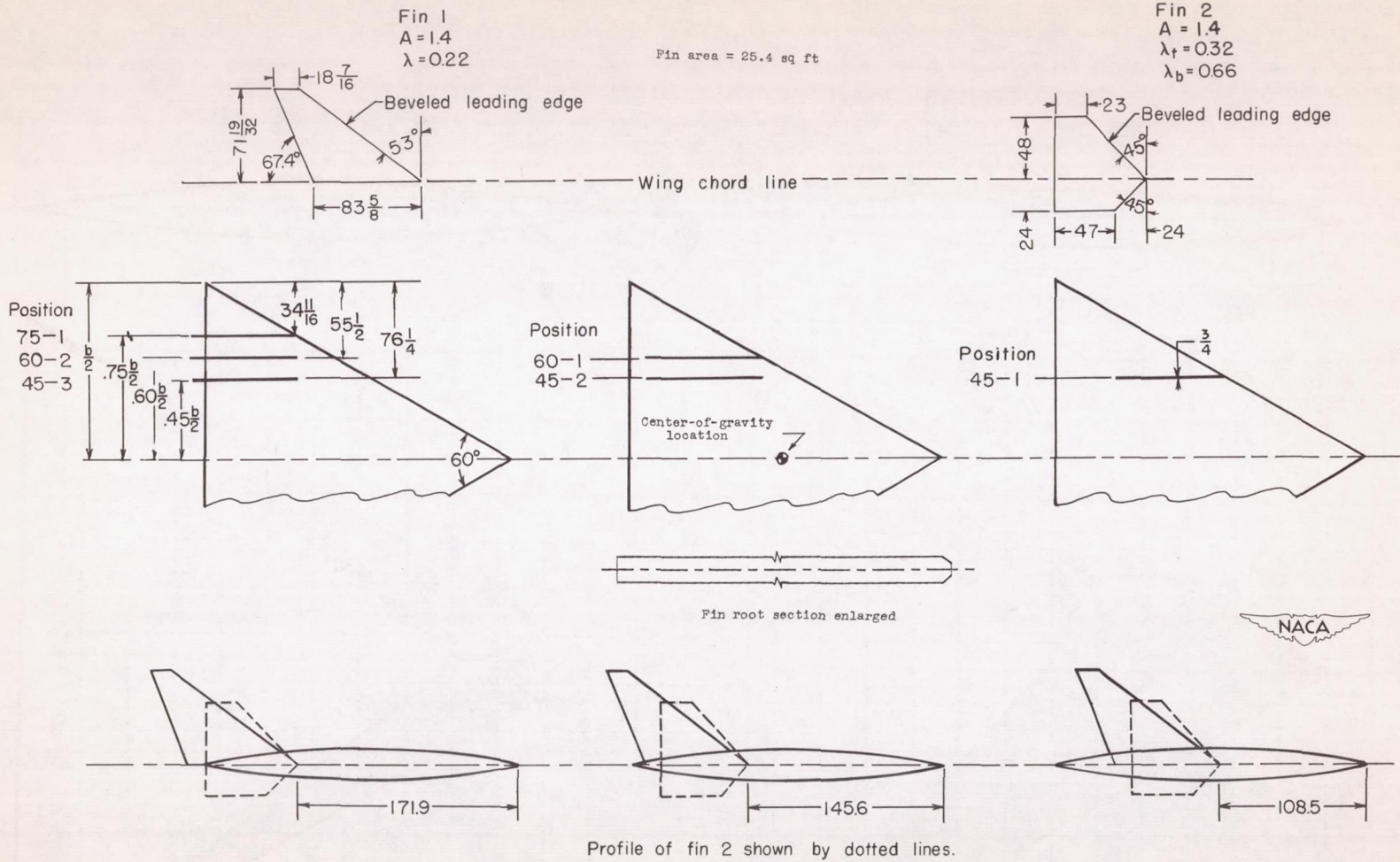
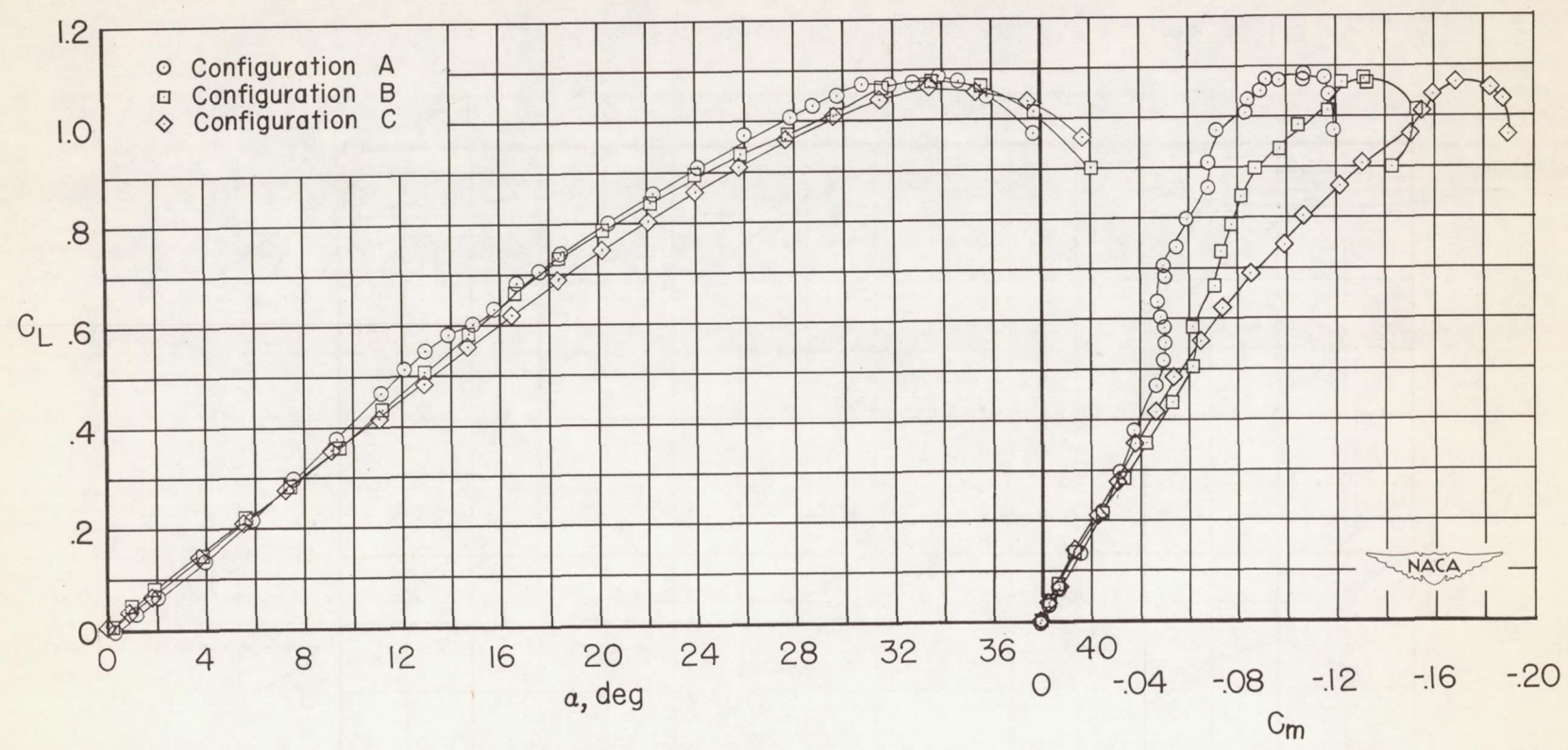
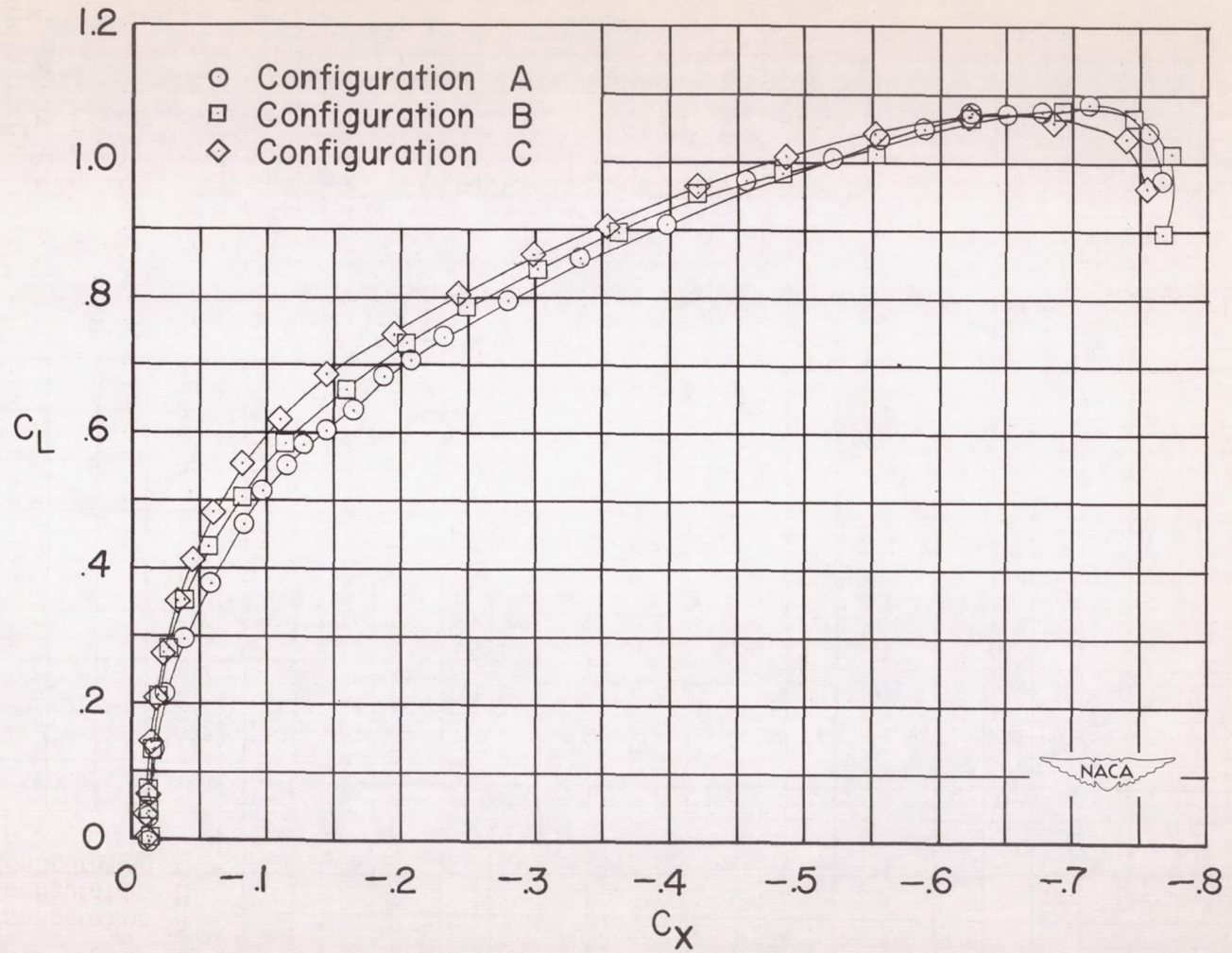


Figure 5.- Geometric characteristics of the fins and the various positions investigated. All dimensions are given in inches. $\frac{S_f}{S_w} = 0.11$. Fins installed on configuration A.



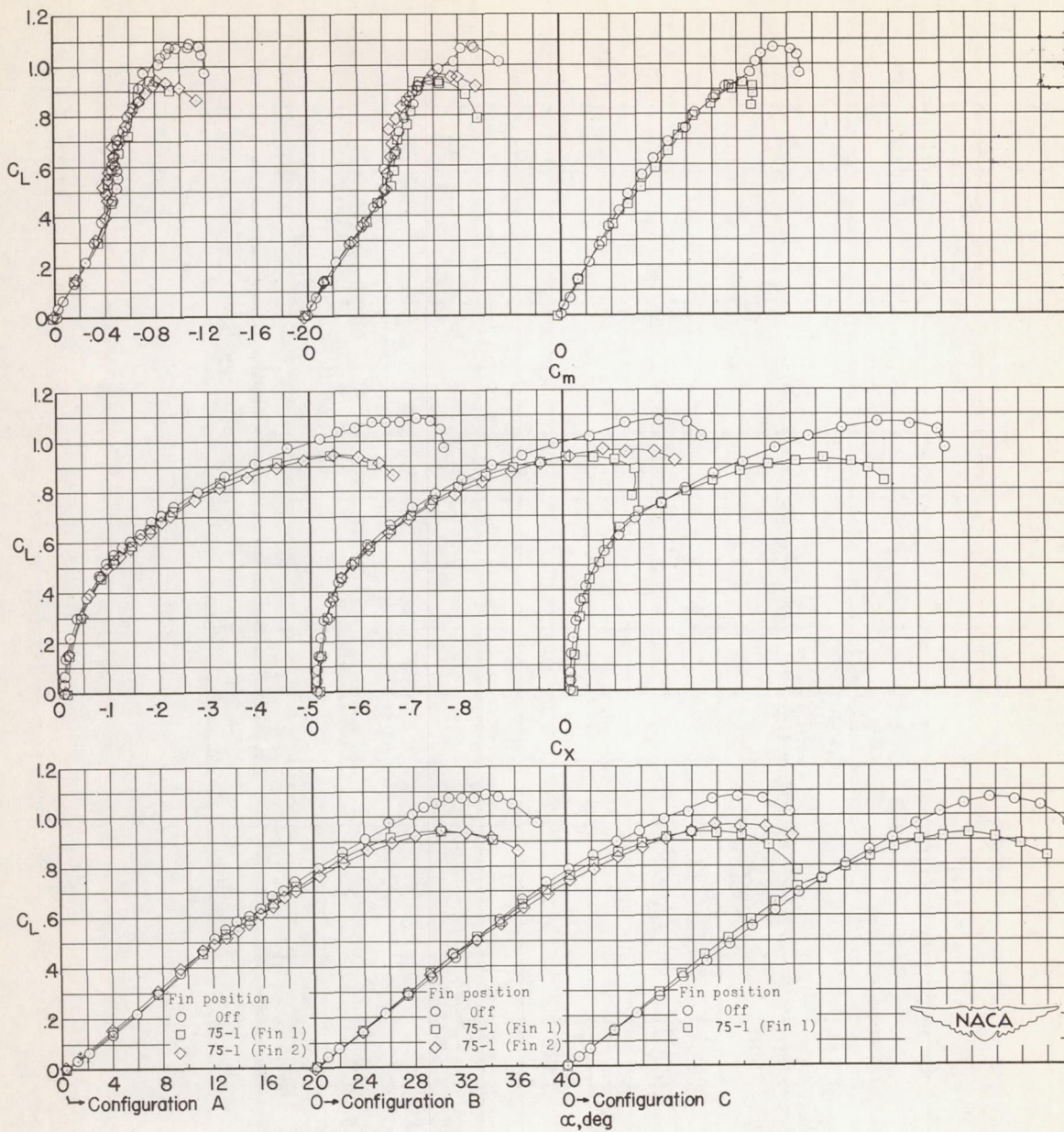
(a) α , C_m against C_L .

Figure 6.- The variations of α , C_x , and C_m with C_L for the three configurations investigated. $R \approx 6.0 \times 10^6$.



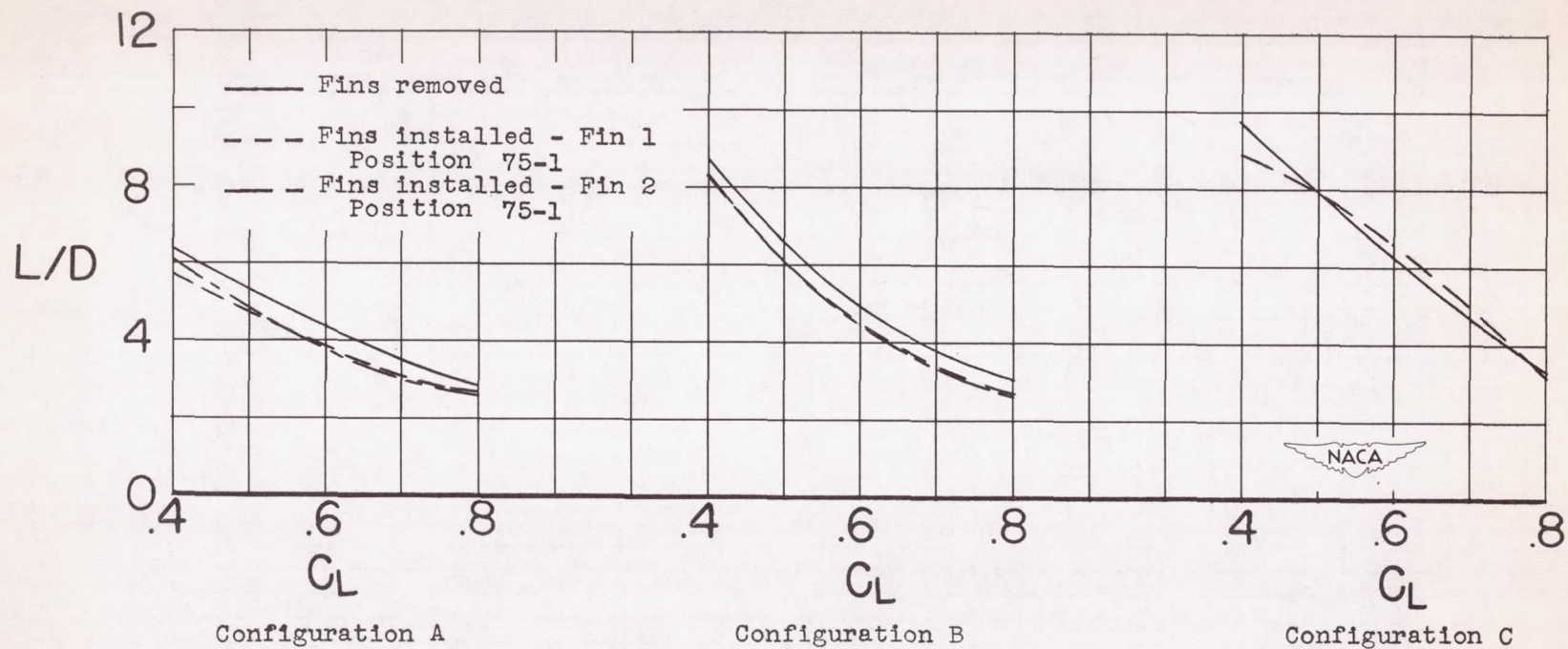
(b) C_x against C_L .

Figure 6.- Concluded.



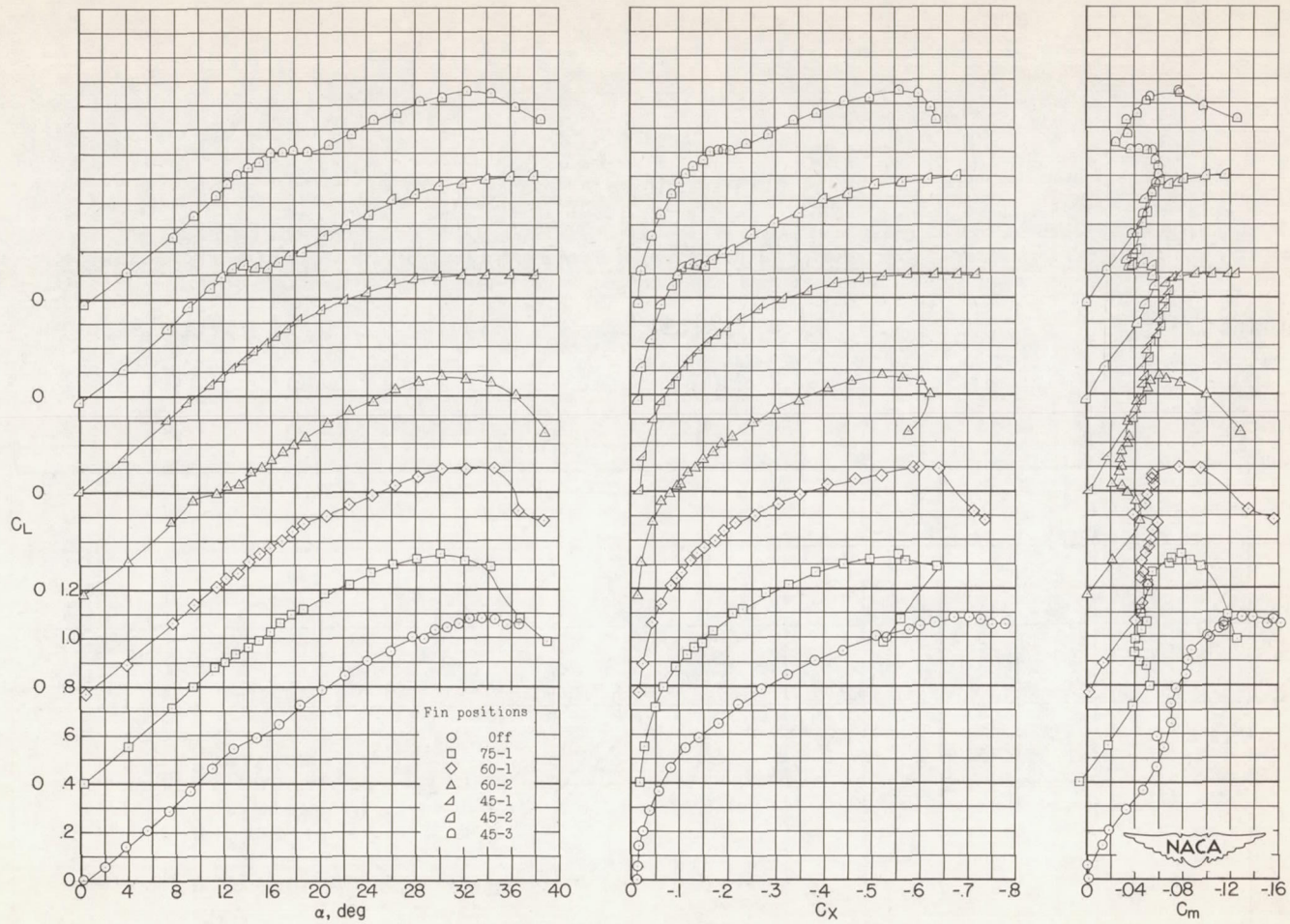
(a) α , C_x , and C_m against C_L .

Figure 7.- The longitudinal aerodynamic characteristics of configurations A, B, and C with fins installed in the most desirable position. $R \approx 6.0 \times 10^6$.



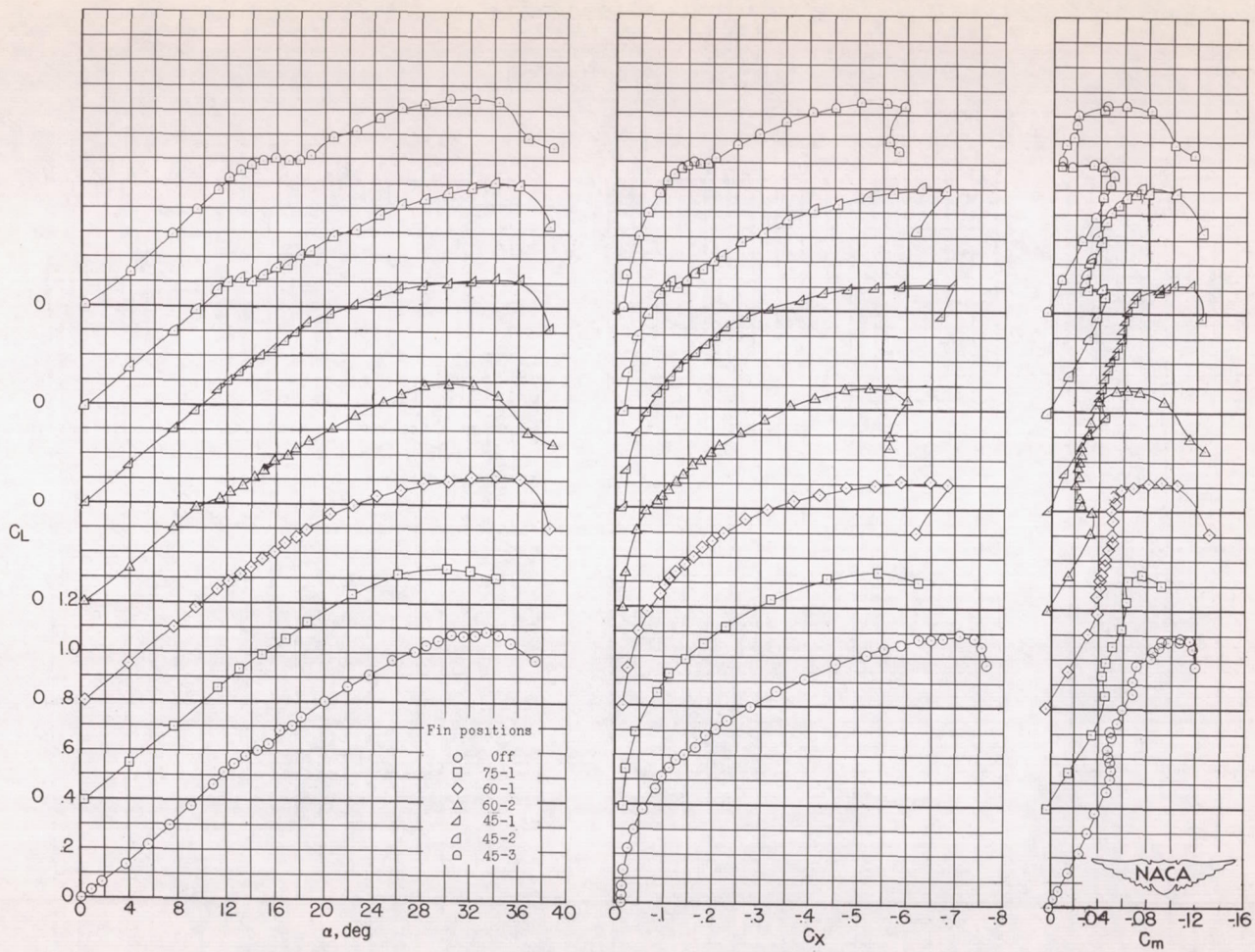
(b) L/D against C_L .

Figure 7.- Concluded.



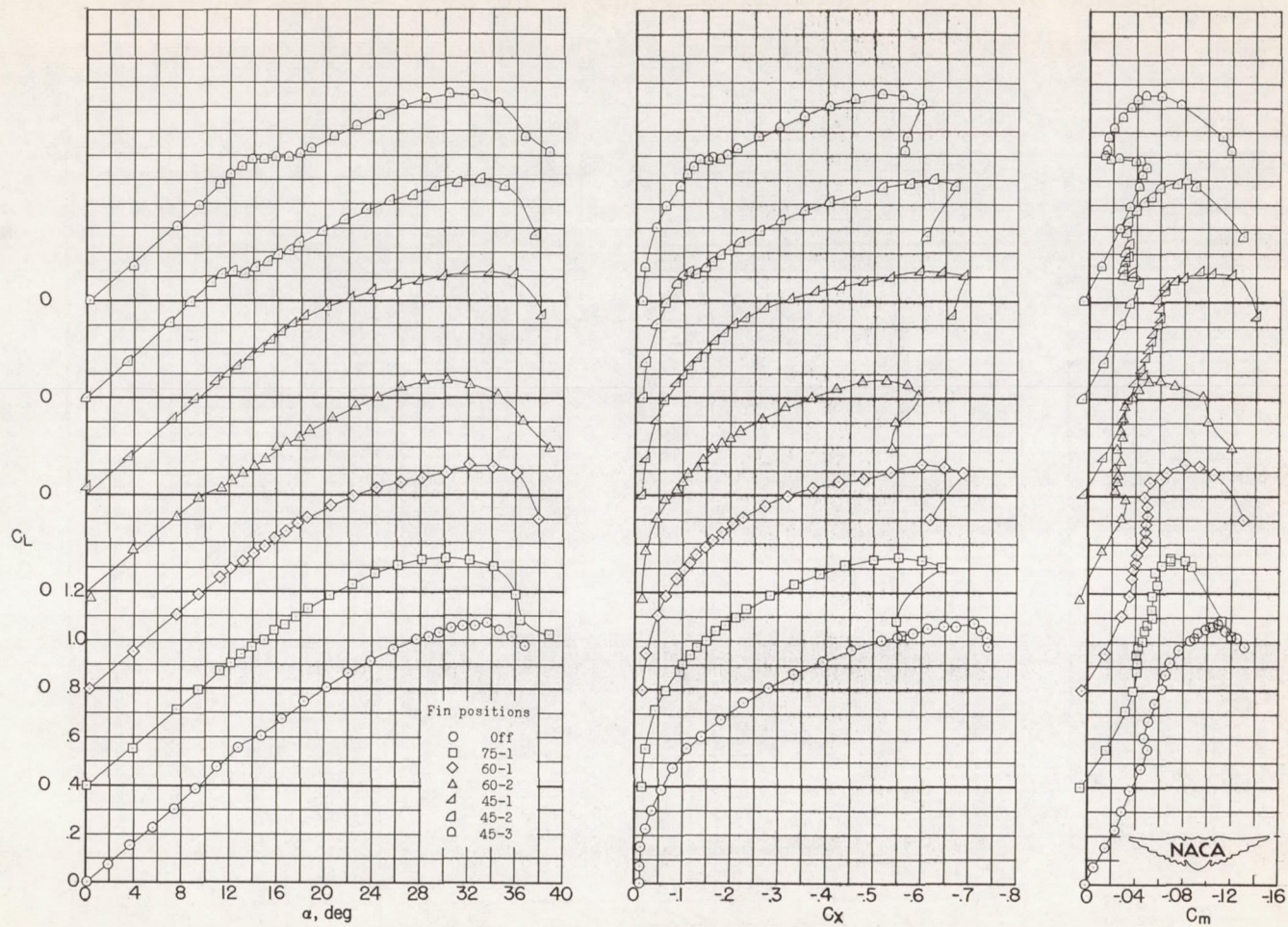
(a) $R \approx 2.9 \times 10^6$.

Figure 8.- Effect of fins and fin positioning on the variations of α , C_x , and C_m with C_L . Configuration A; fin 1.



(b) $R \approx 6.0 \times 10^6$.

Figure 8.- Continued.



(c) $R \approx 9.7 \times 10^6$.

Figure 8.- Concluded.

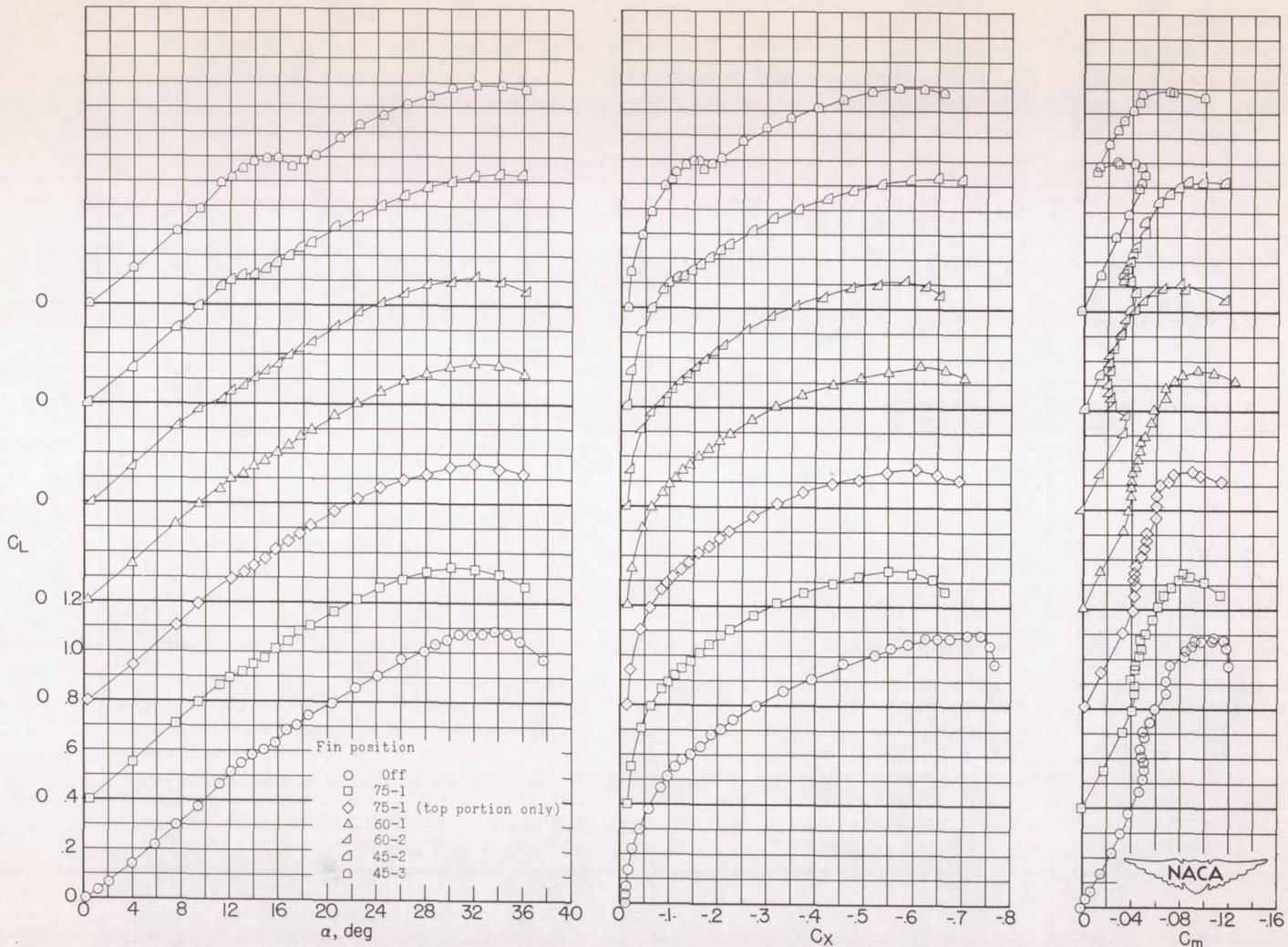
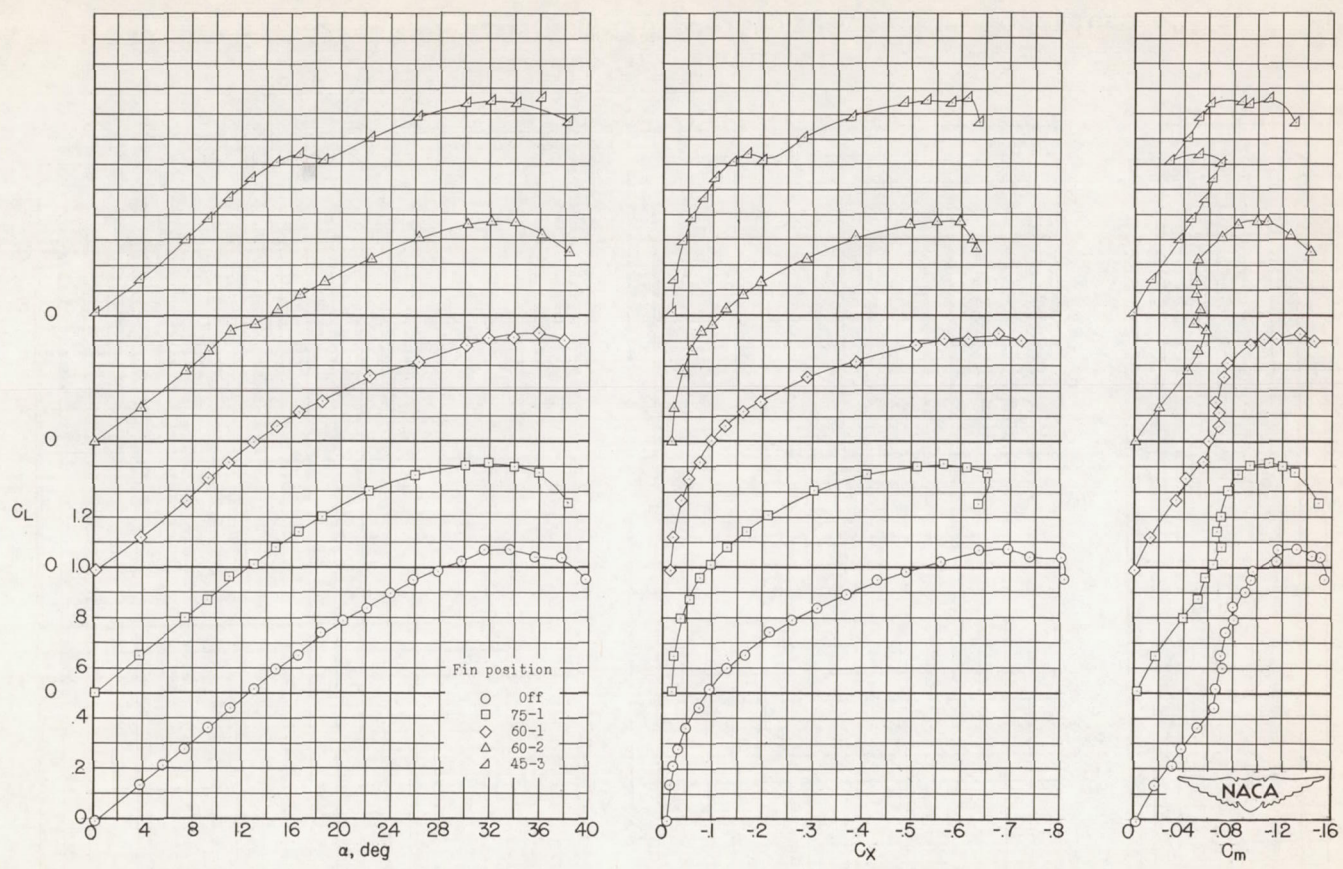
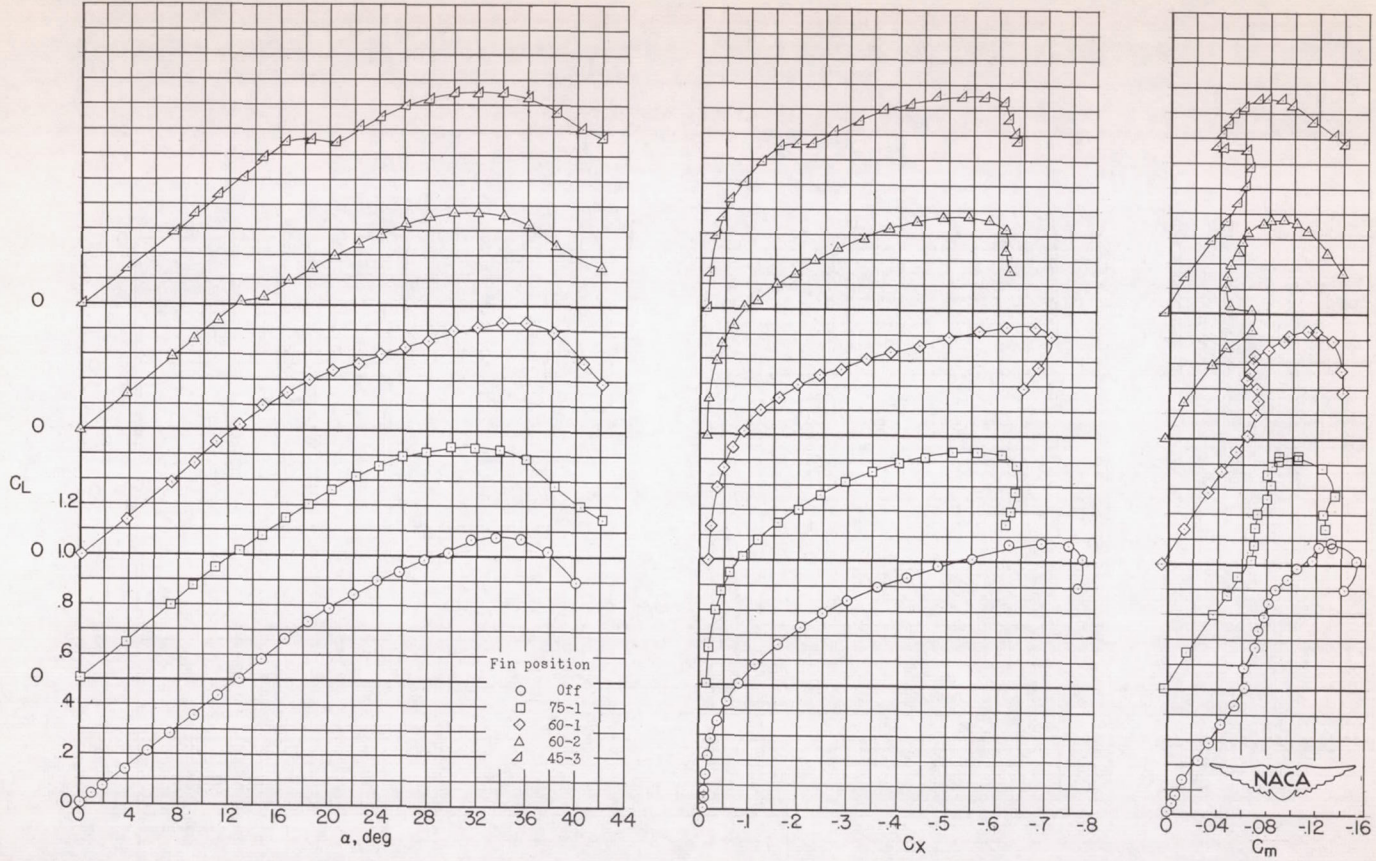


Figure 9.- Effect of fins and fin positioning on the variations of α , C_x , and C_m with C_L . Configuration A; fin 2. $R \approx 6.0 \times 10^6$.



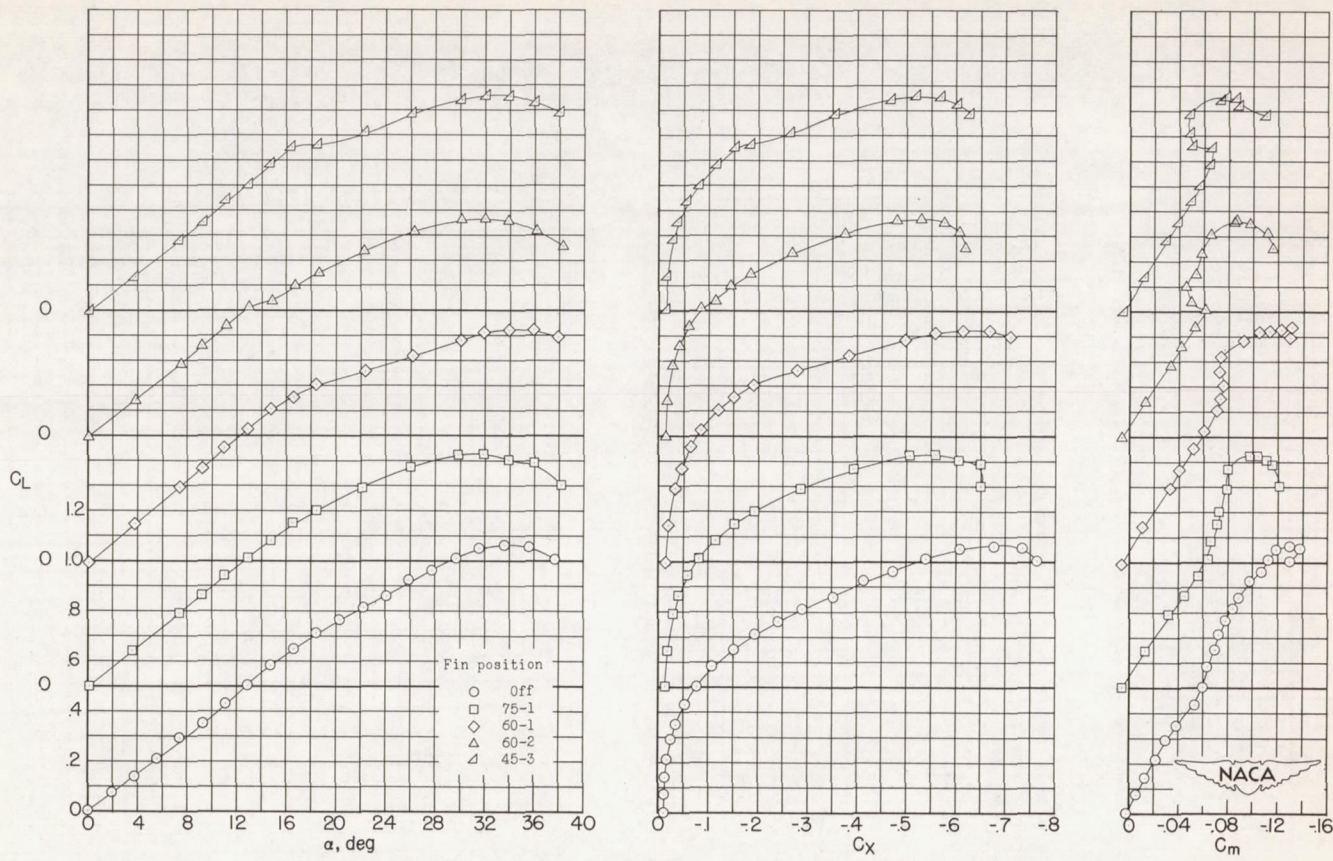
(a) $R \approx 2.9 \times 10^6$.

Figure 10.- Effect of fins and fin positioning on the variations of α , C_x , and C_m with C_L . Configuration B; fin 1.



(b) $R \approx 6.0 \times 10^6$.

Figure 10.- Continued.



(c) $R \approx 9.7 \times 10^6$.

Figure 10.- Concluded.

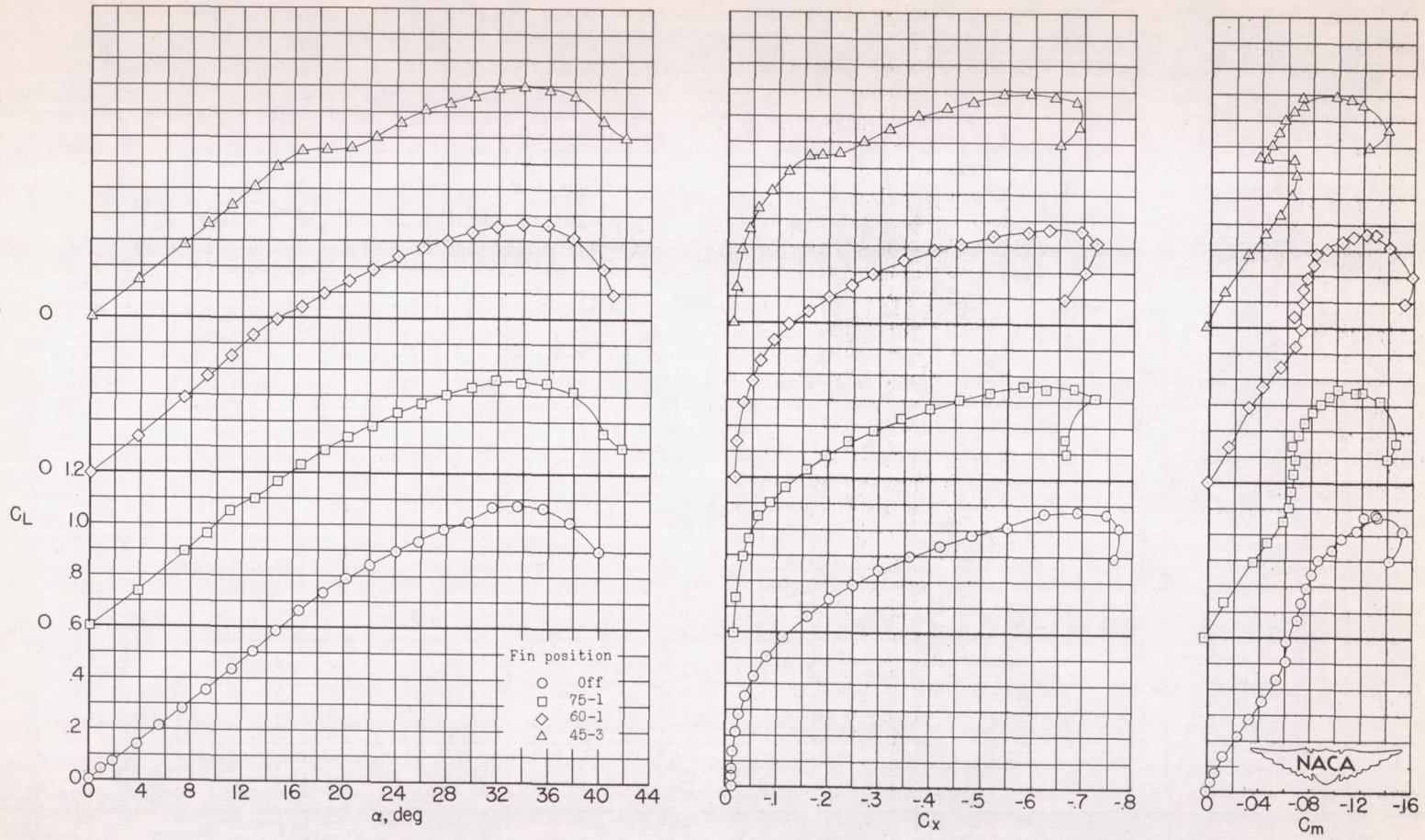
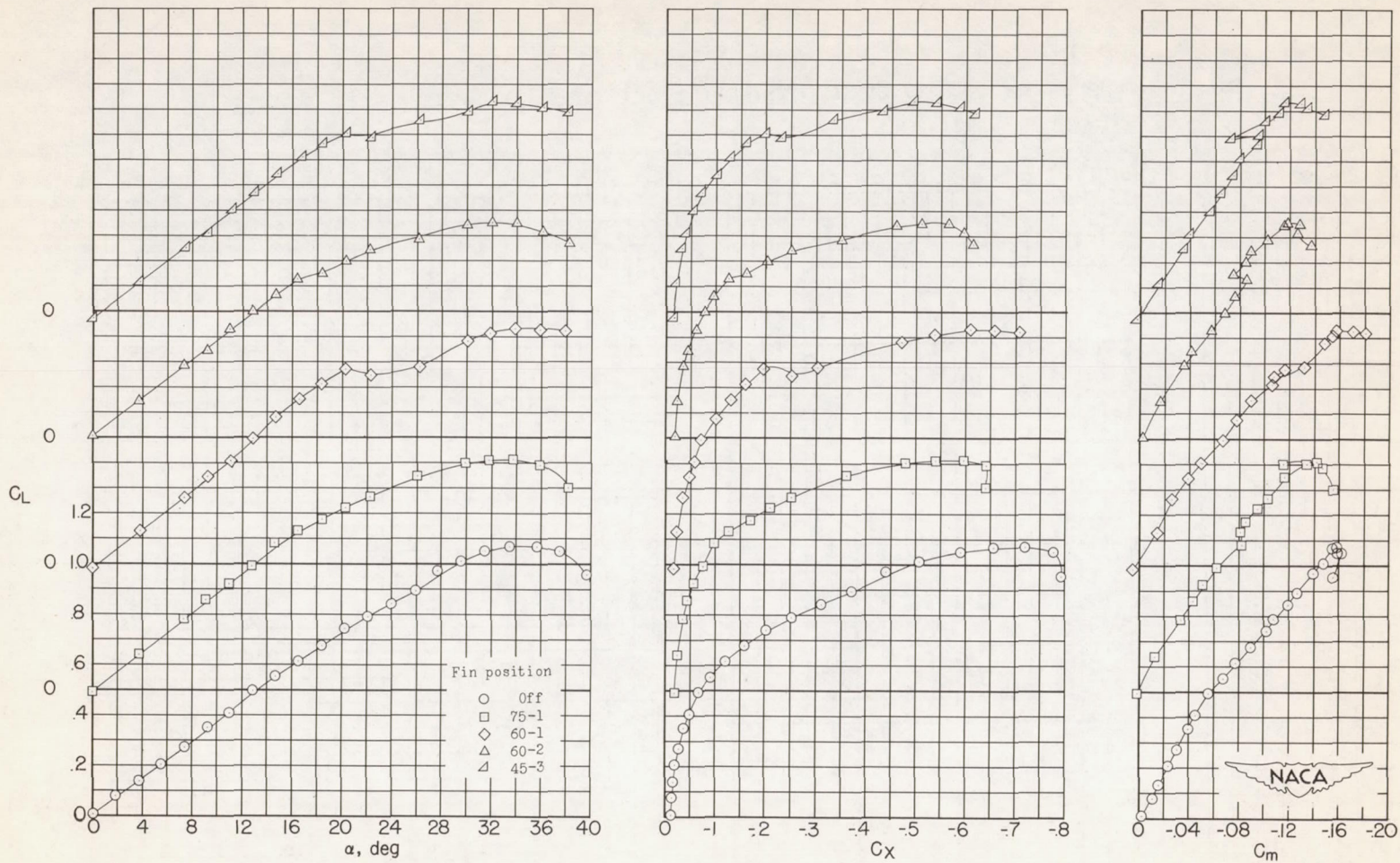
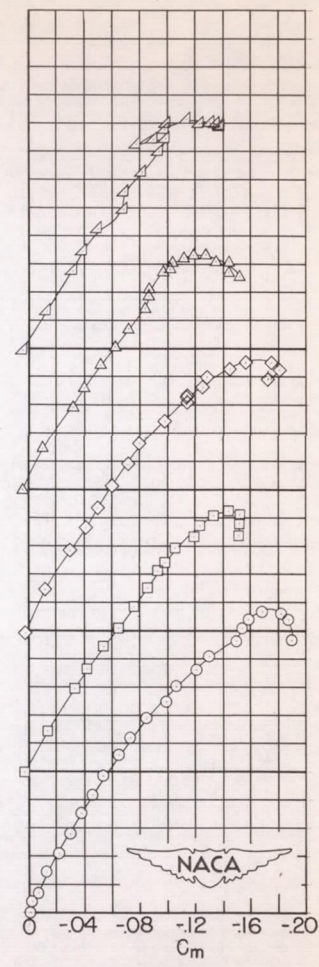
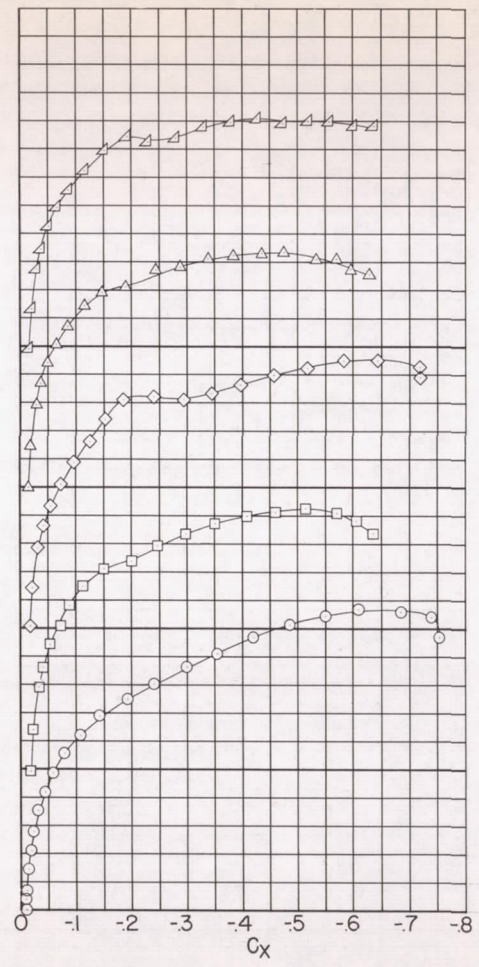
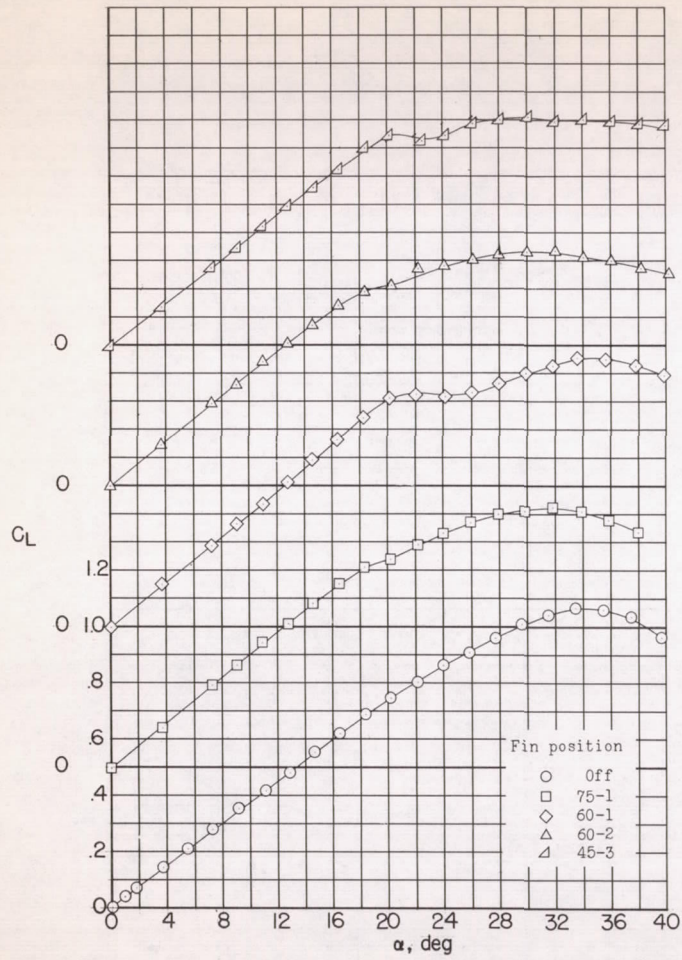


Figure 11.- Effect of fins and fin positioning on the variations of α , C_x , and C_m with C_L . Configuration B; fin 2. $R \approx 6.0 \times 10^6$.



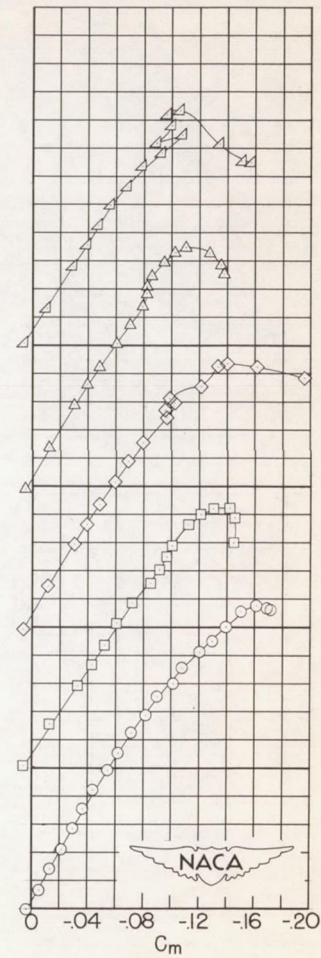
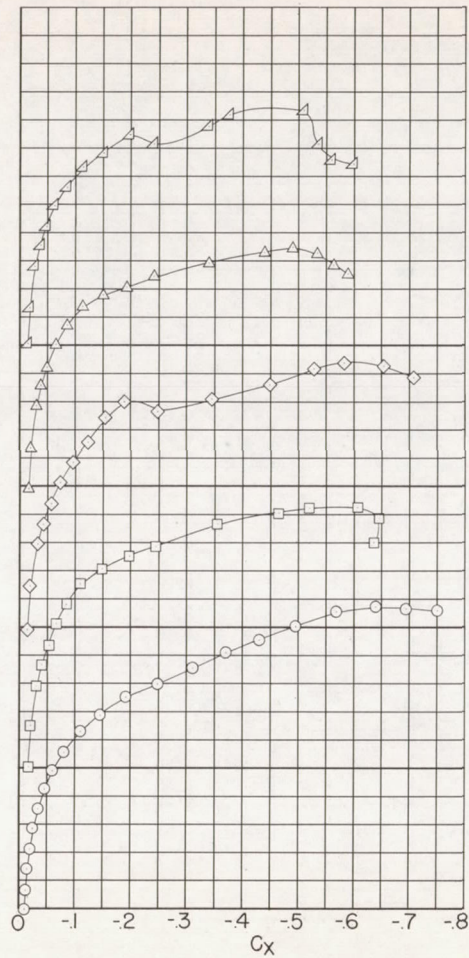
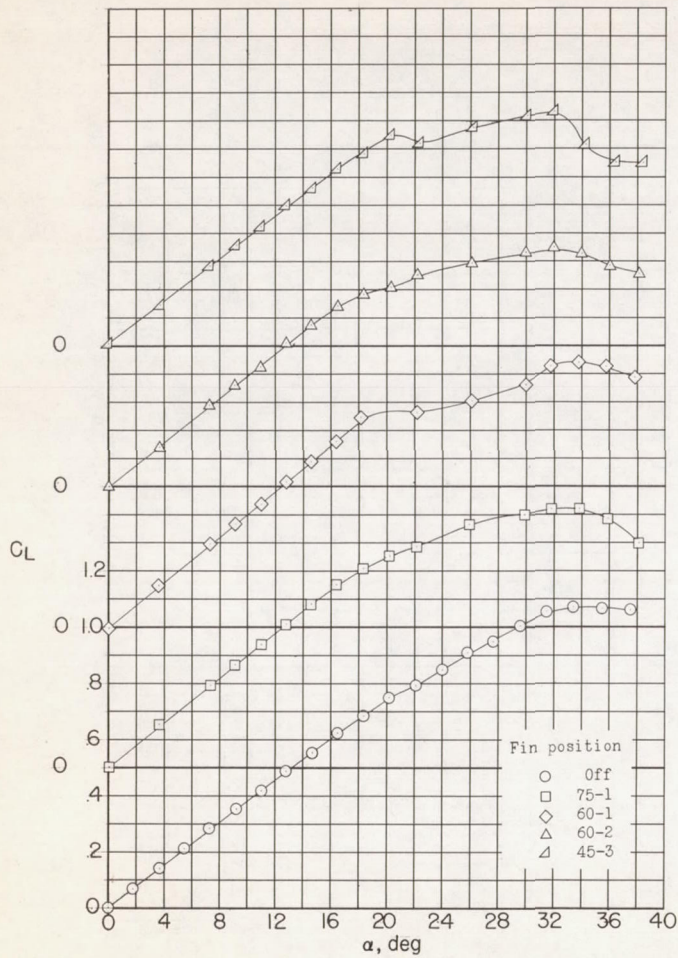
(a) $R \approx 2.9 \times 10^6$.

Figure 12.- Effect of fins and fin positioning on the variations of α , C_X , and C_M with C_L . Configuration C; fin 1.



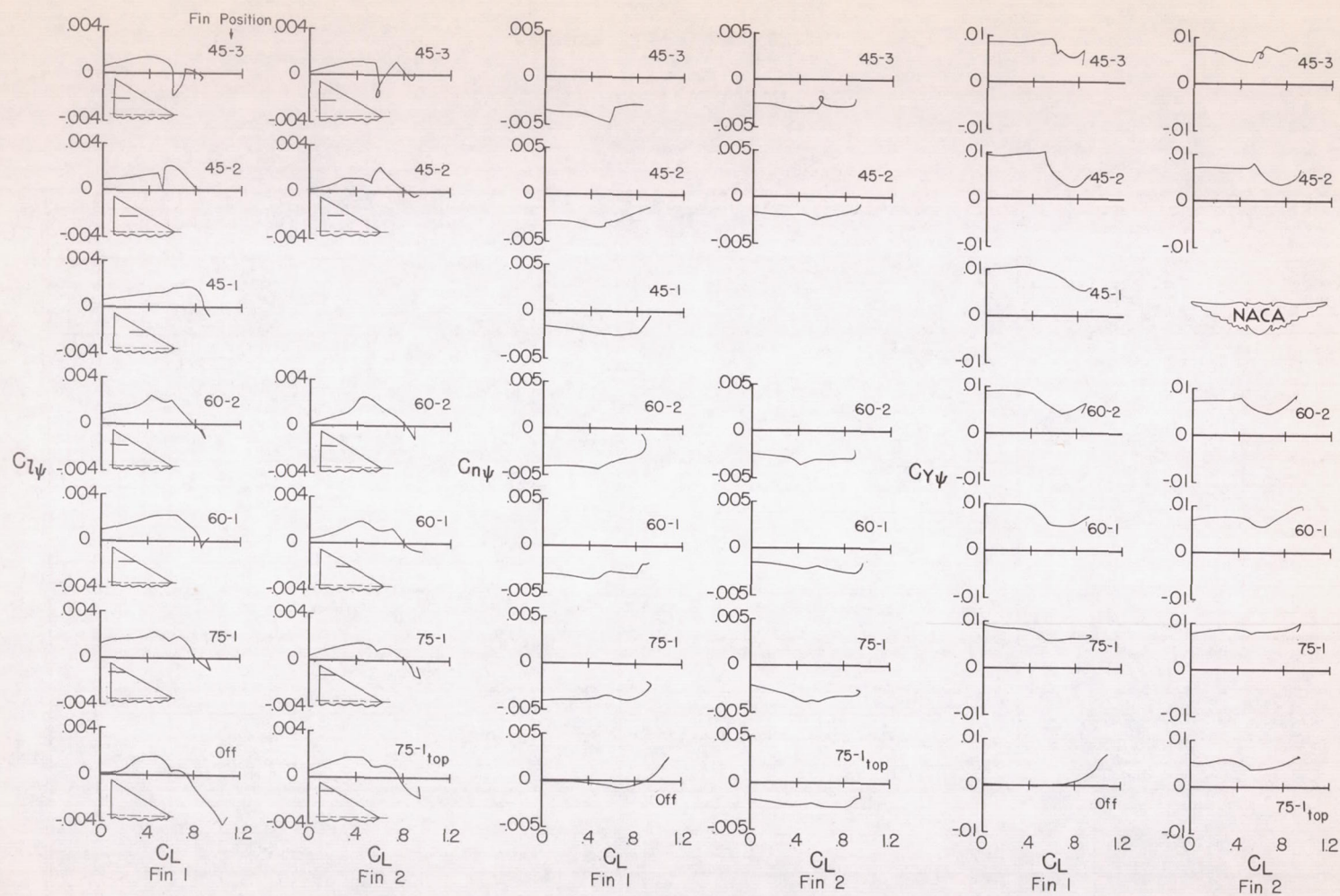
(b) $R \approx 6.0 \times 10^6$.

Figure 12.- Continued.



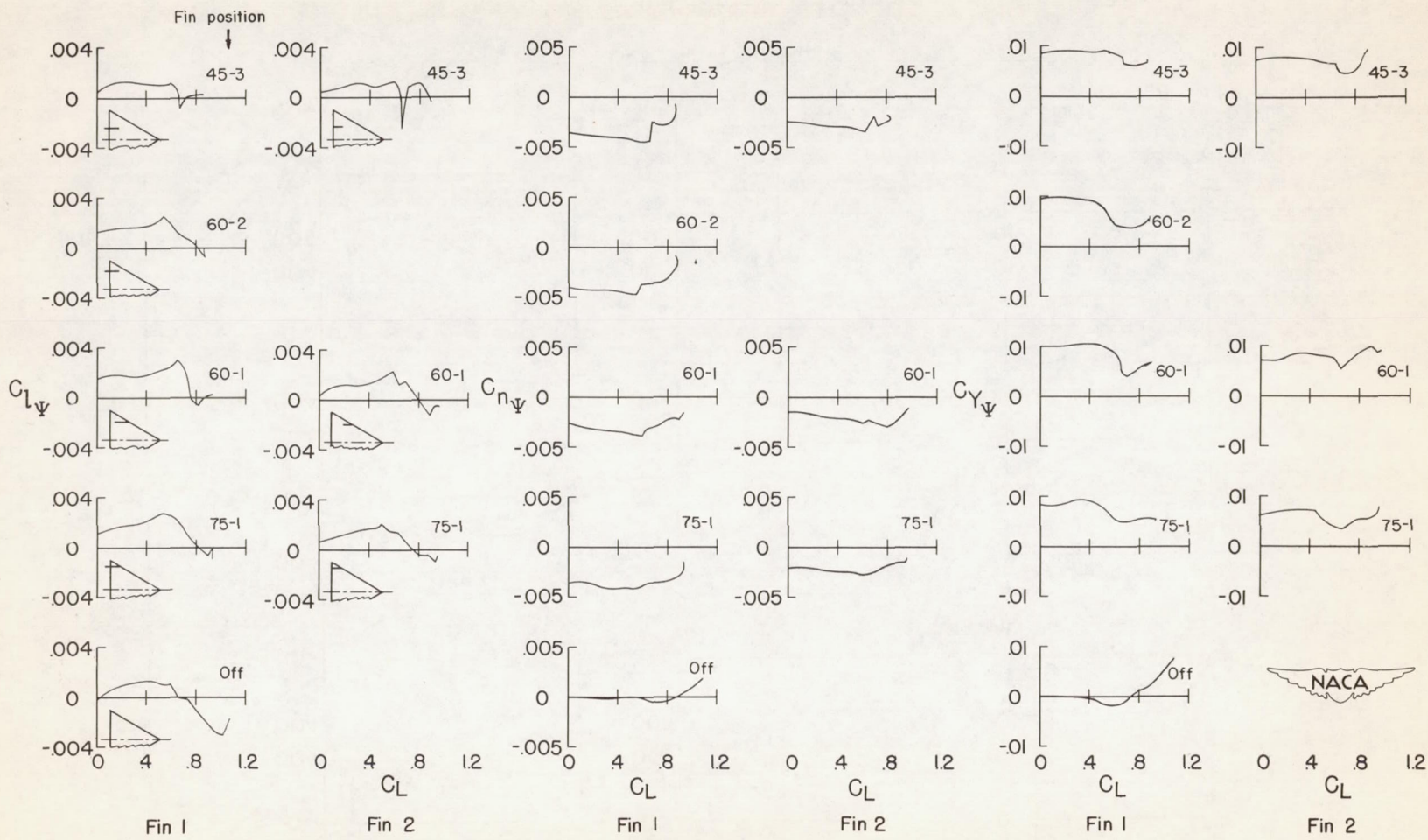
(c) $R \approx 9.7 \times 10^6$.

Figure 12.- Concluded.



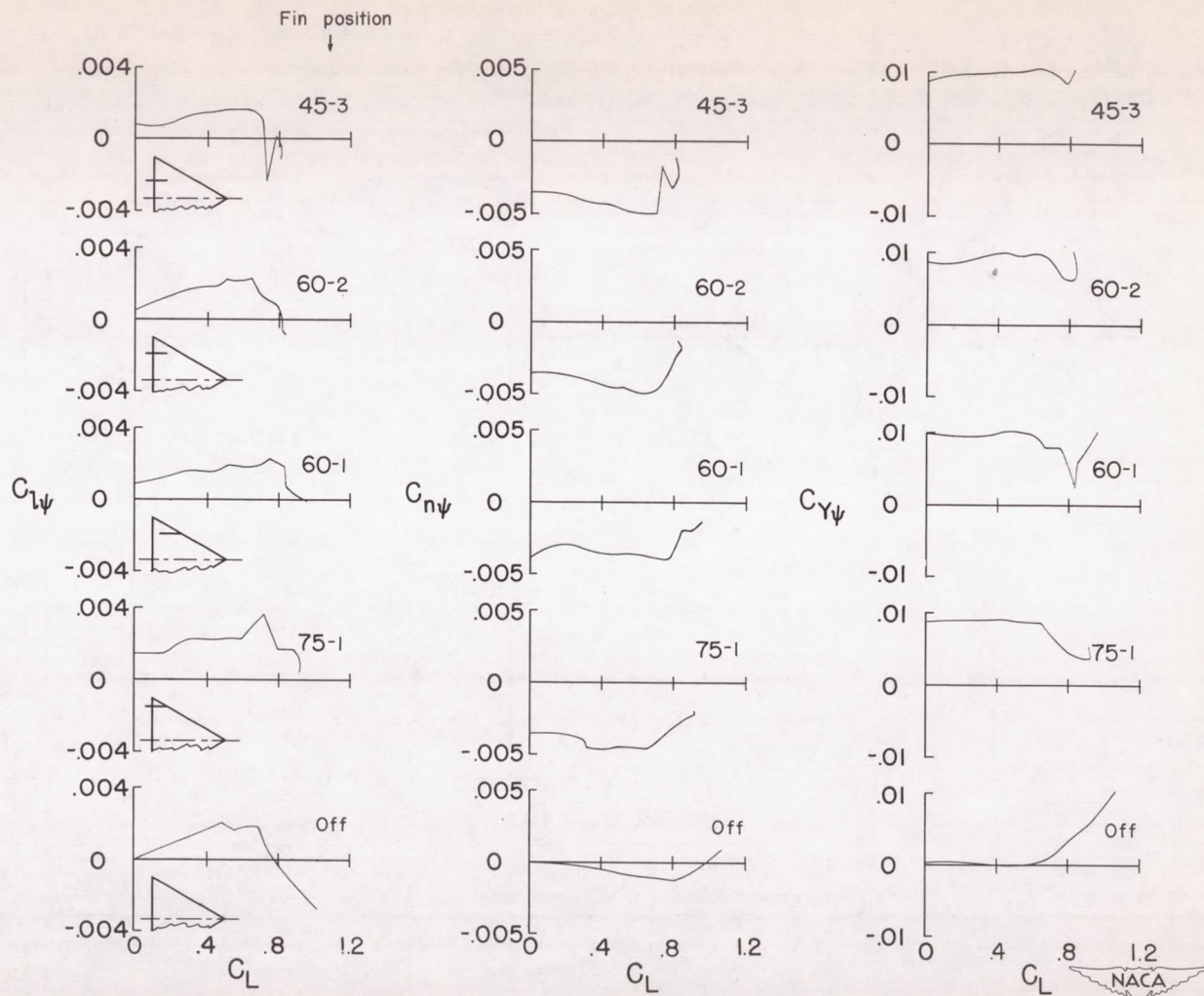
(a) Configuration A.

Figure 13.- Effect of fins and fin positioning on the static lateral stability characteristics. $R \approx 6.0 \times 10^6$.



(b) Configuration B.

Figure 13.- Continued.



(c) Configuration C, fin 1.

Figure 13.- Concluded.

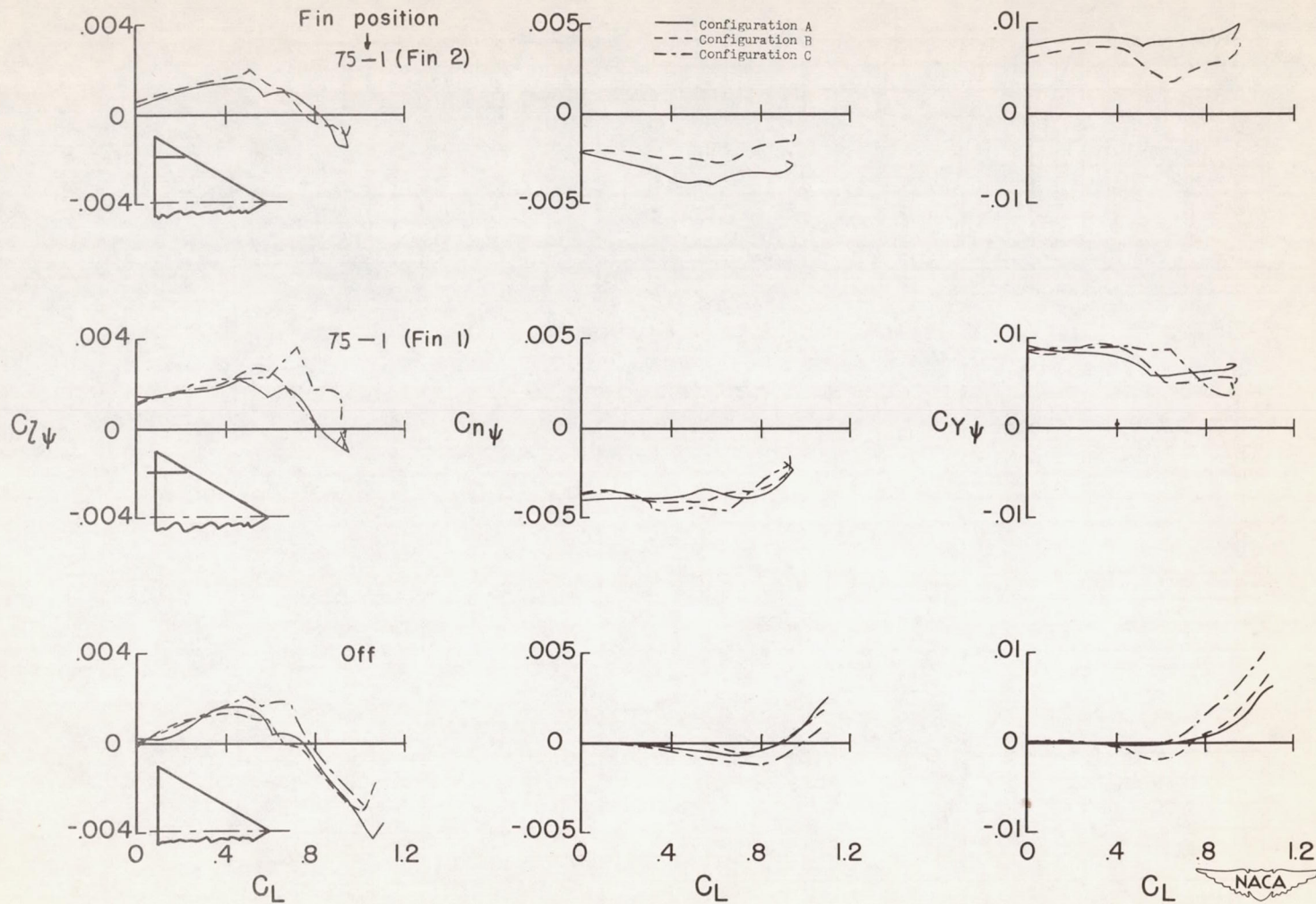
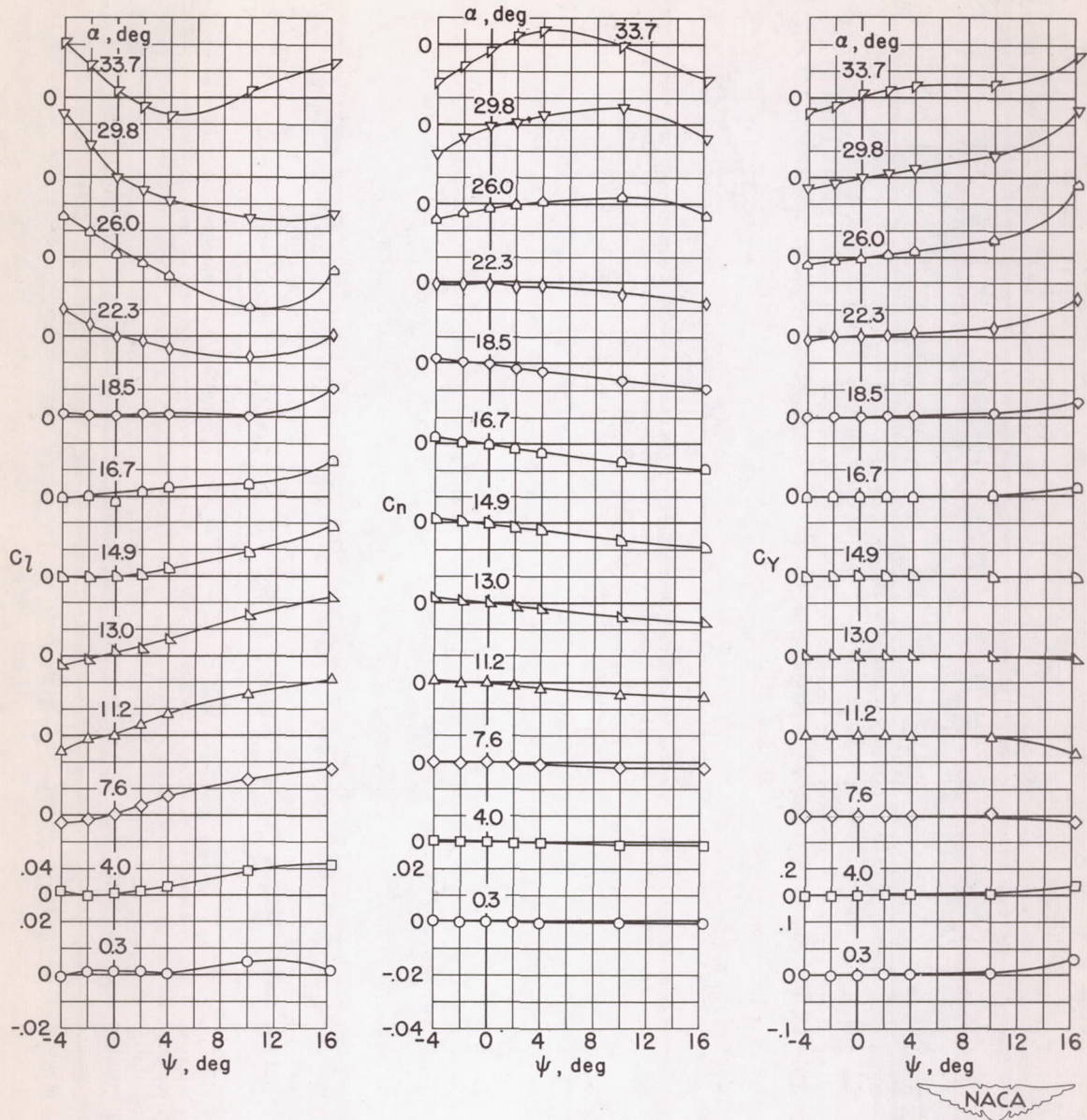
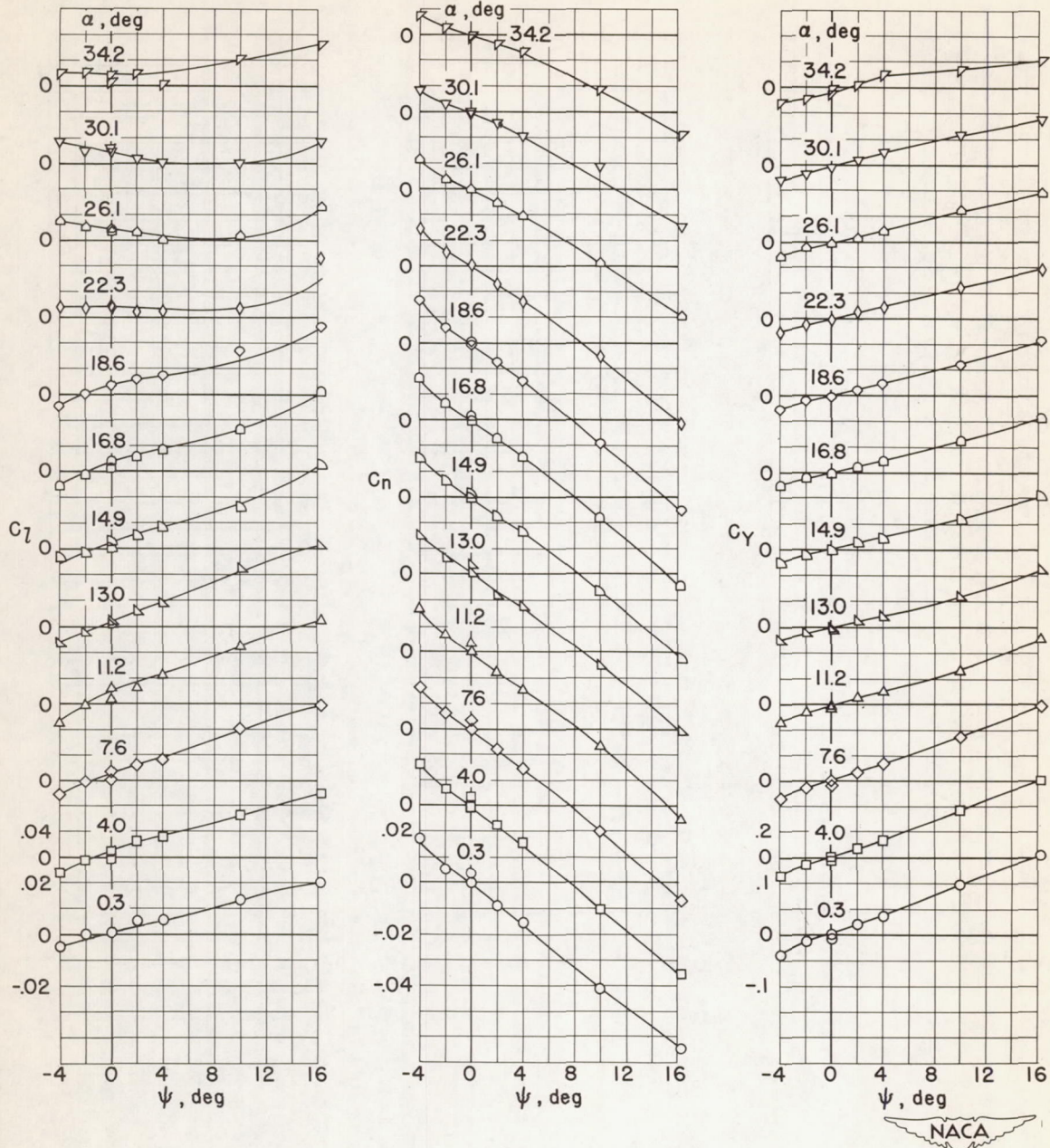


Figure 14.- The effect of wing leading-edge modifications on the lateral stability characteristics with fins removed and installed in the most desirable position of 75-1. $R \approx 6.0 \times 10^6$.



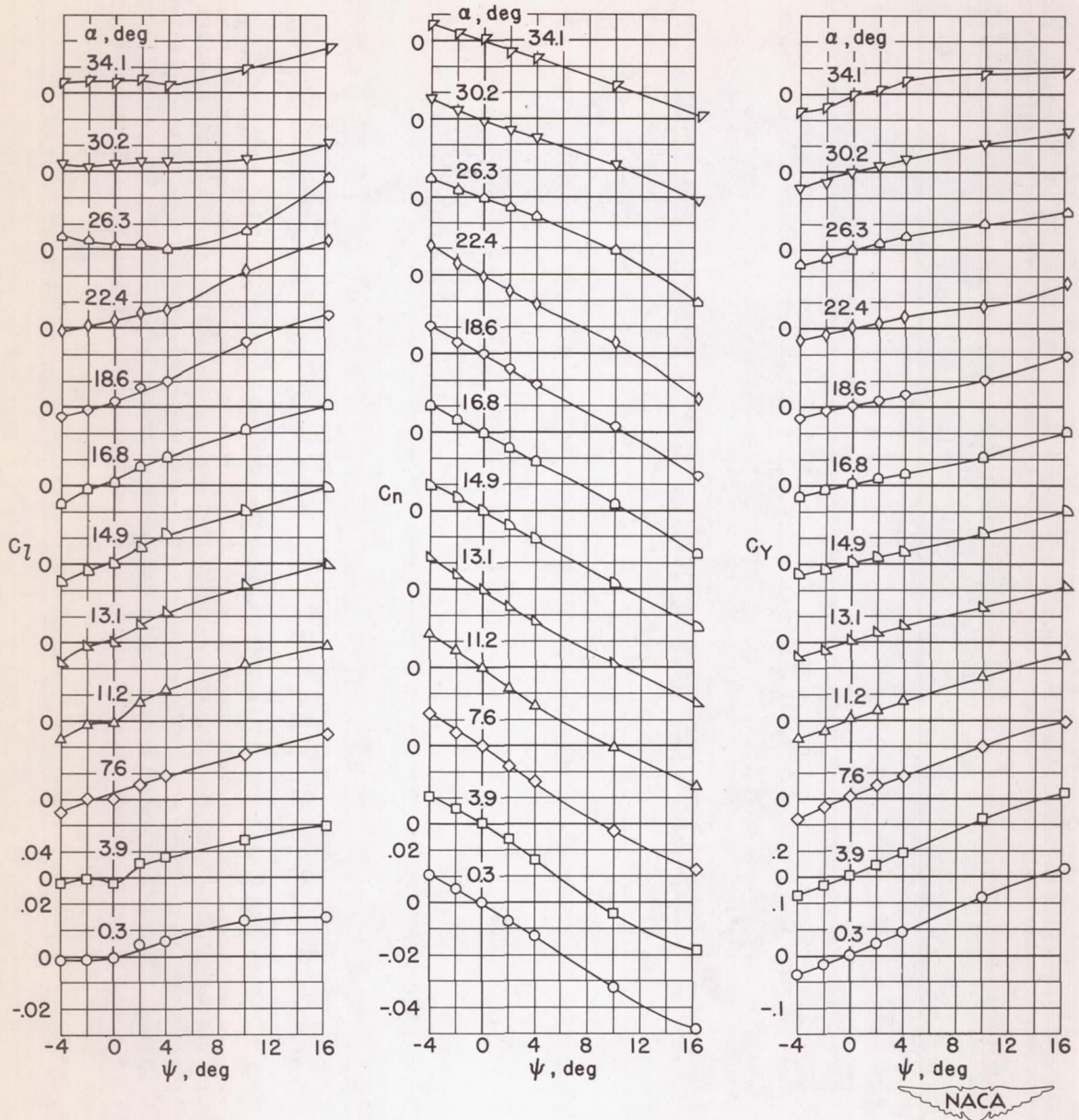
(a) Fins removed.

Figure 15.- The effects of fins and fin positioning on the variations of C_l , C_n , and C_y with ψ . Configuration A, fin 1. $R \approx 6.0 \times 10^6$.



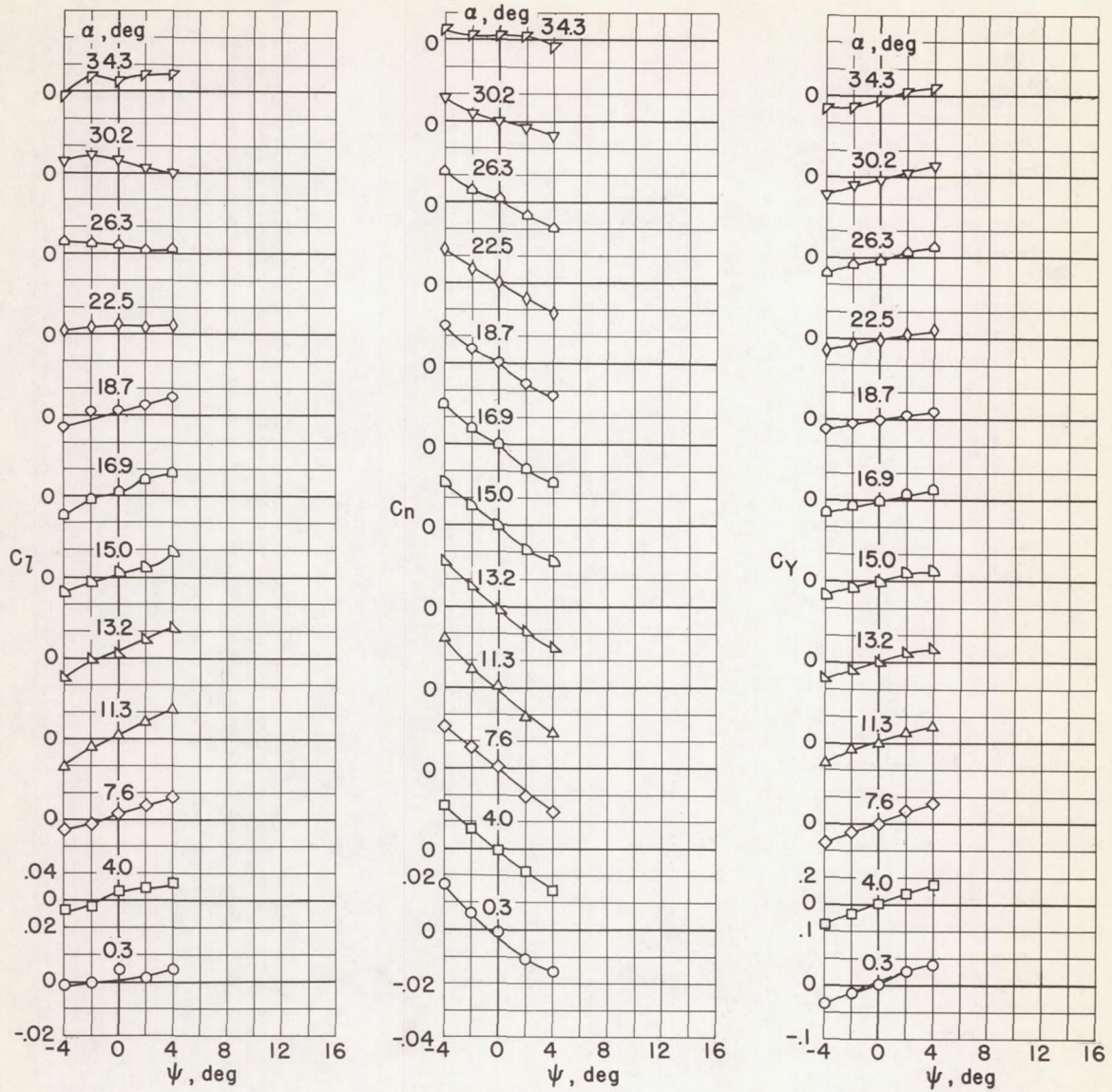
(b) Position 75-1.

Figure 15.- Continued.



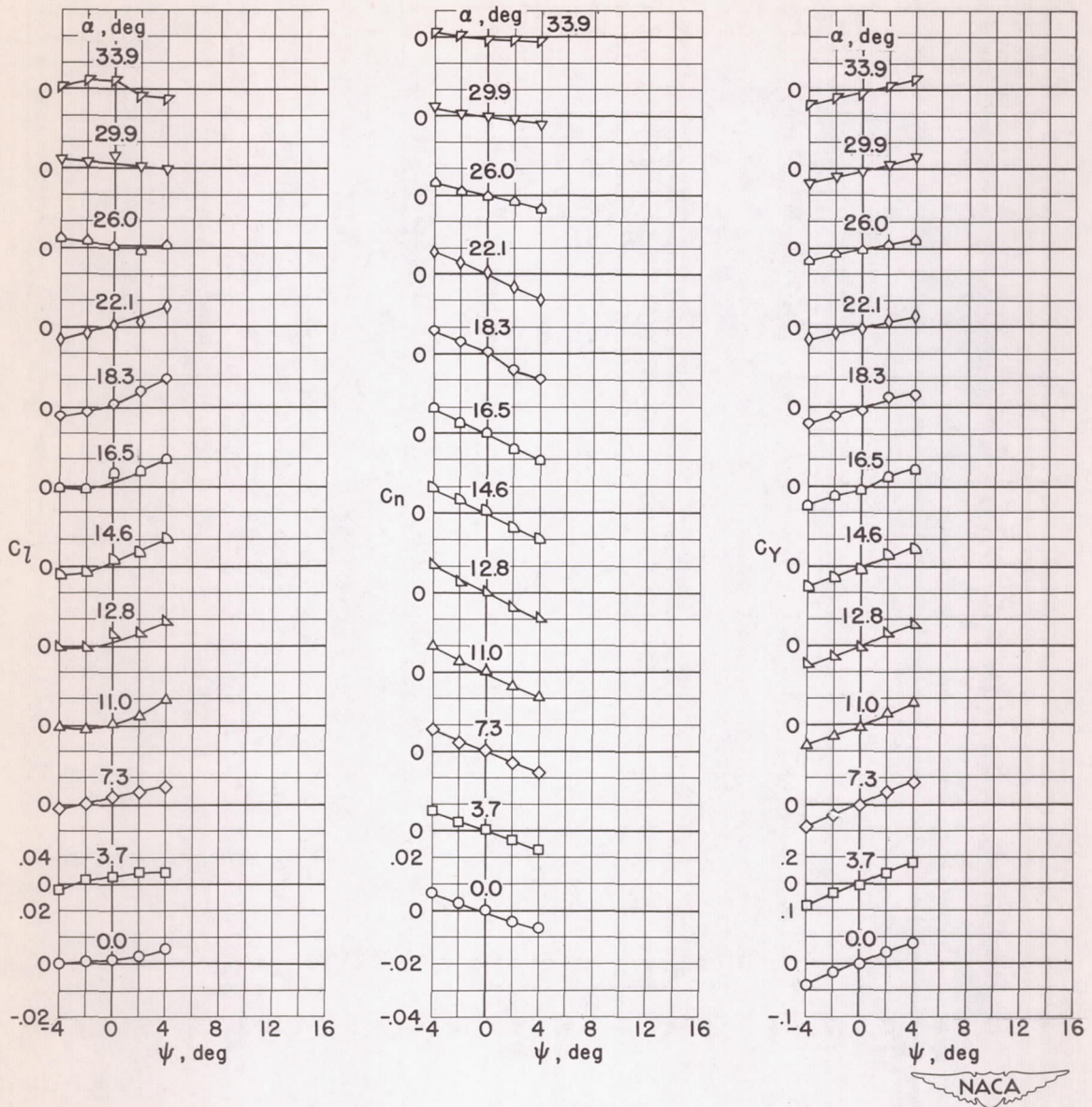
(c) Position 60-1.

Figure 15.- Continued.

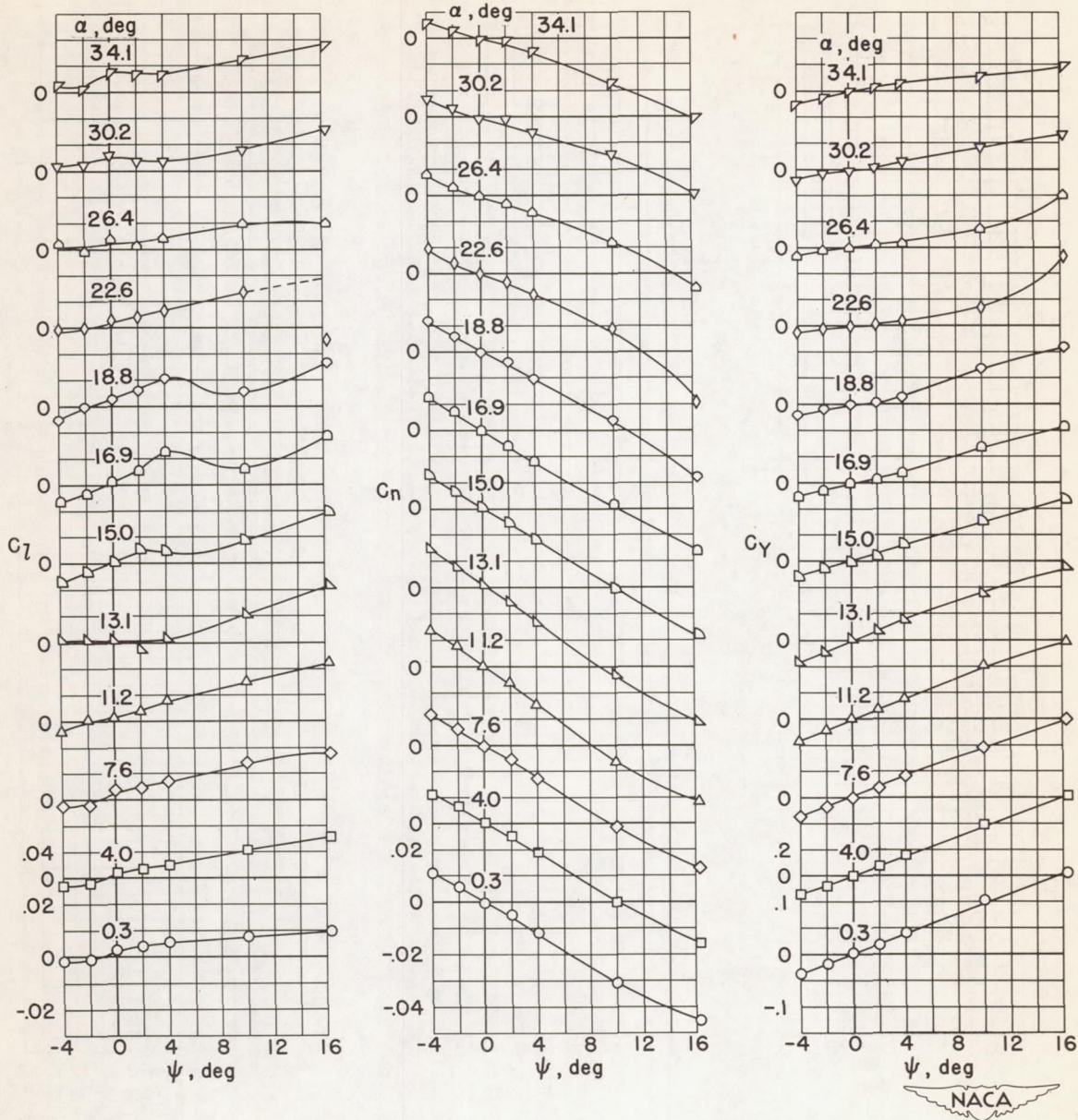


(d) Position 60-2.

Figure 15.- Continued.

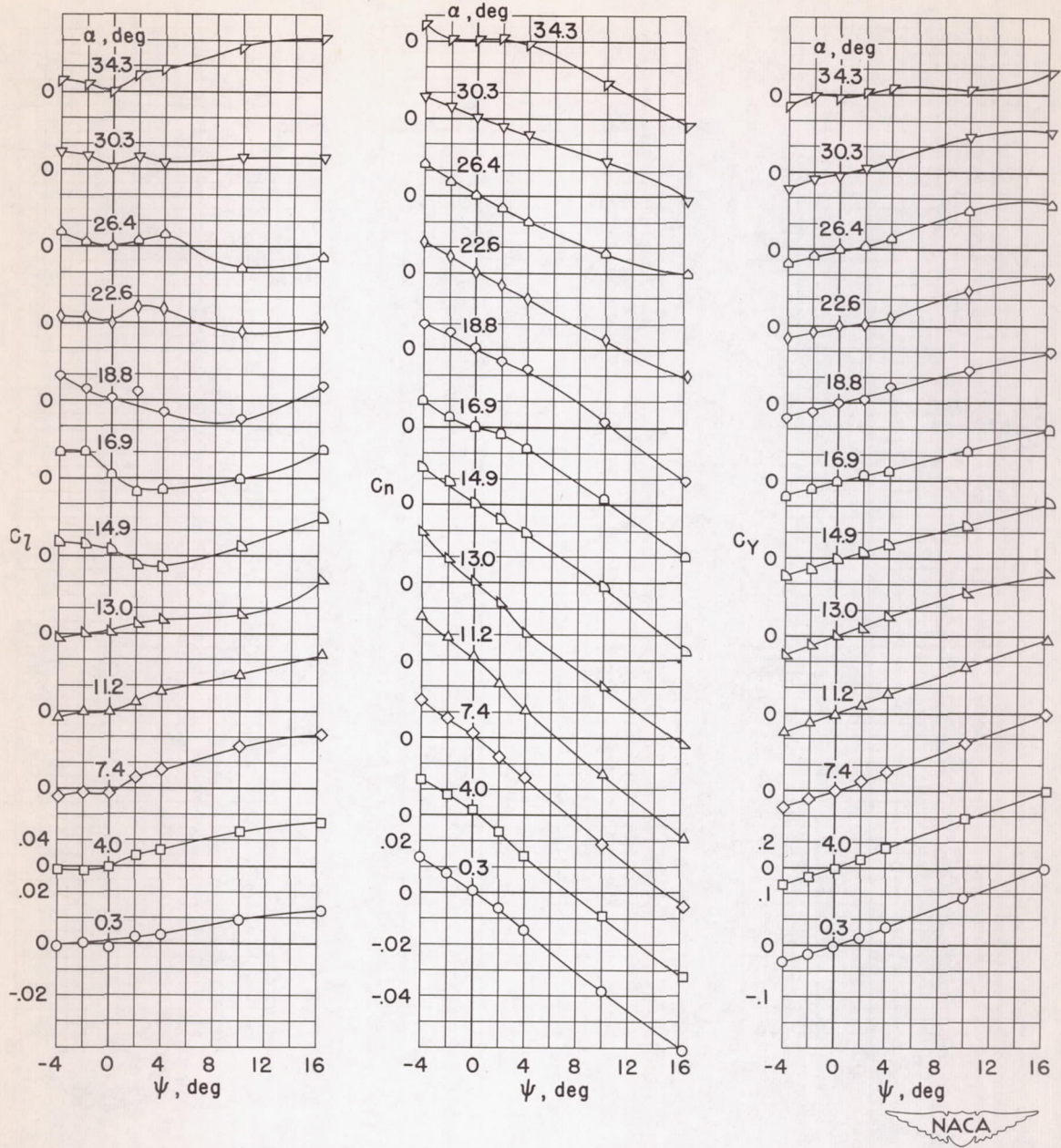


(e) Position 45-1.
 Figure 15.- Continued.



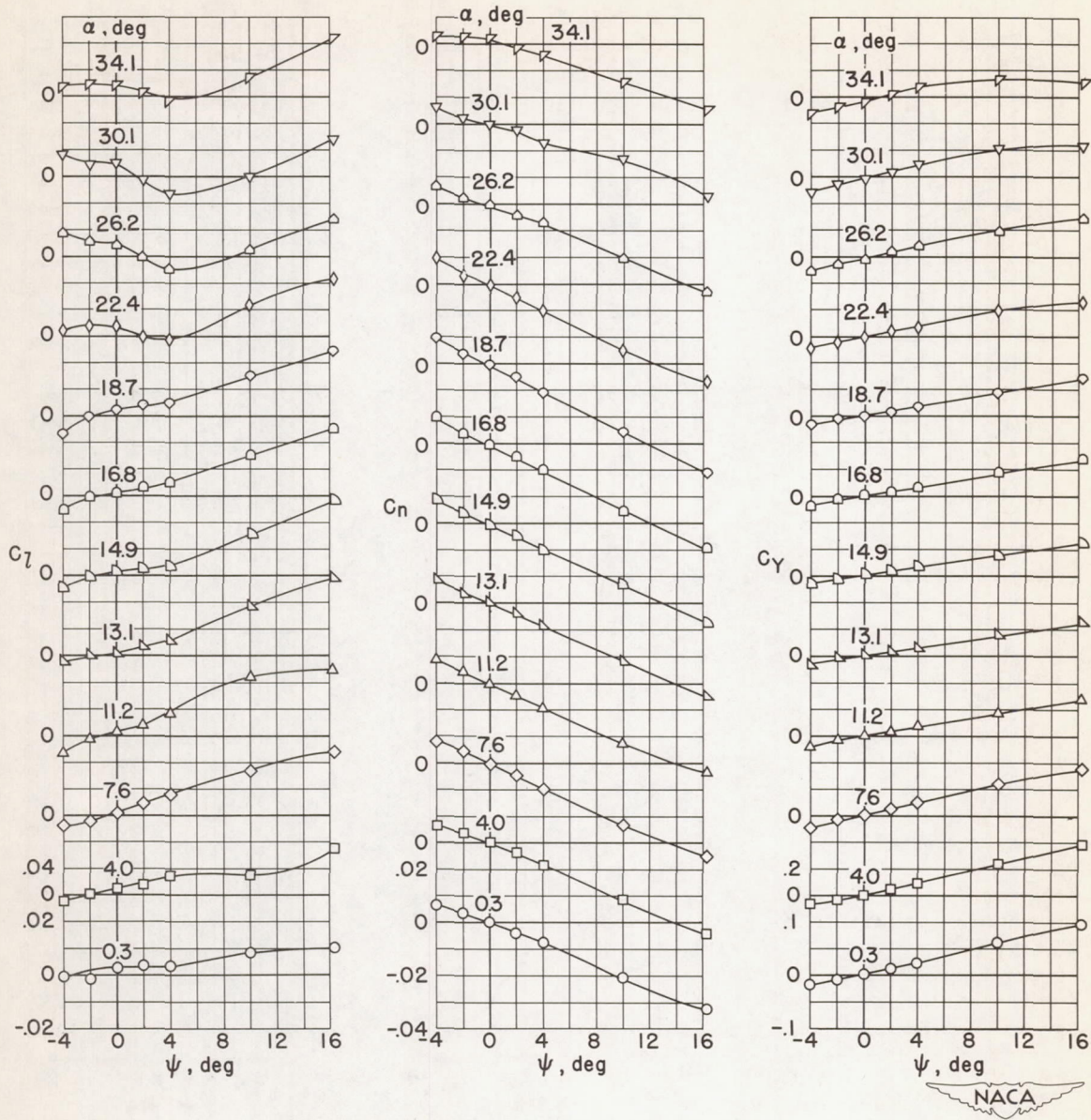
(f) Position 45-2.

Figure 15.- Continued.



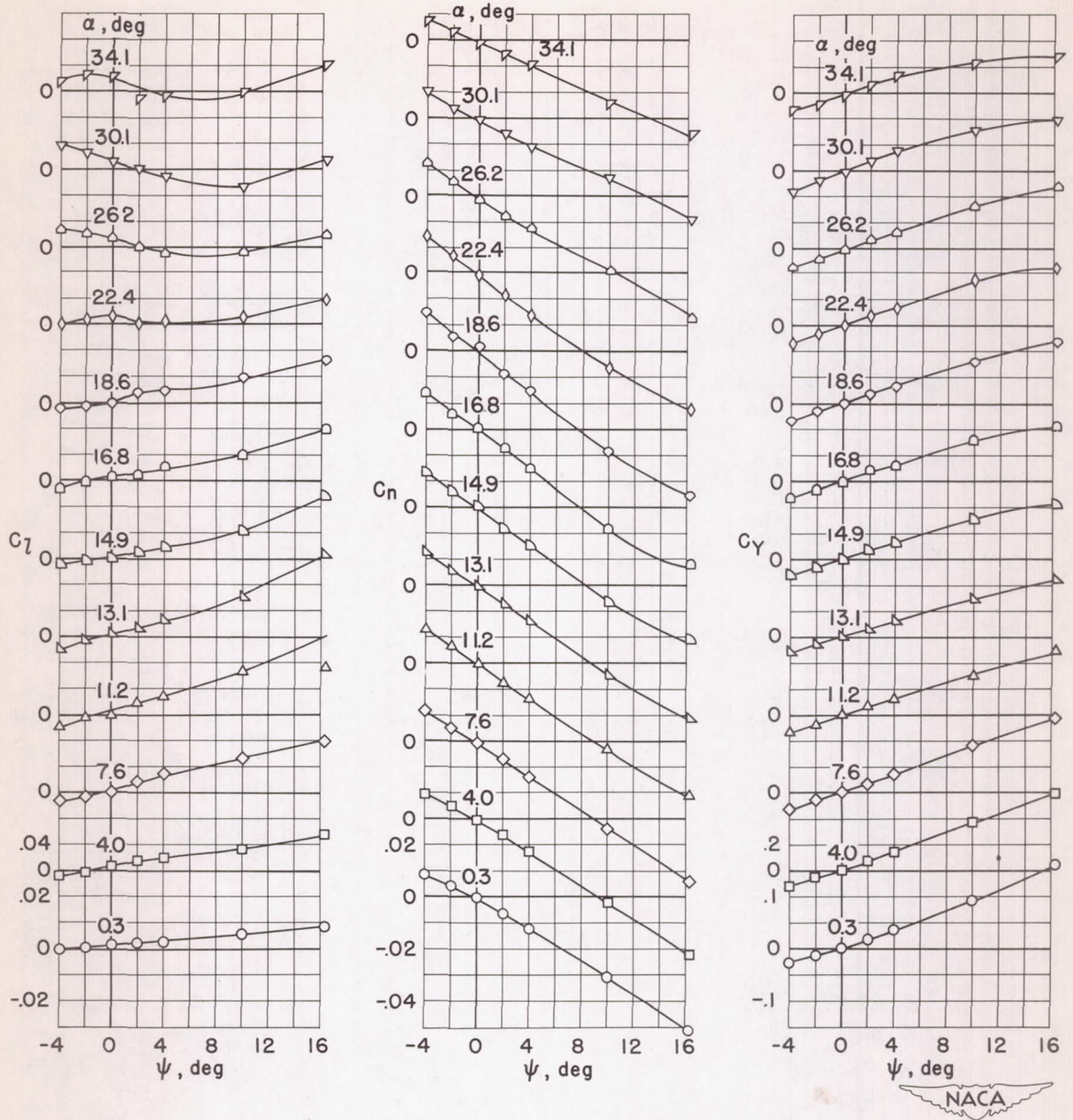
(g) Position 45-3.

Figure 15.- Concluded.



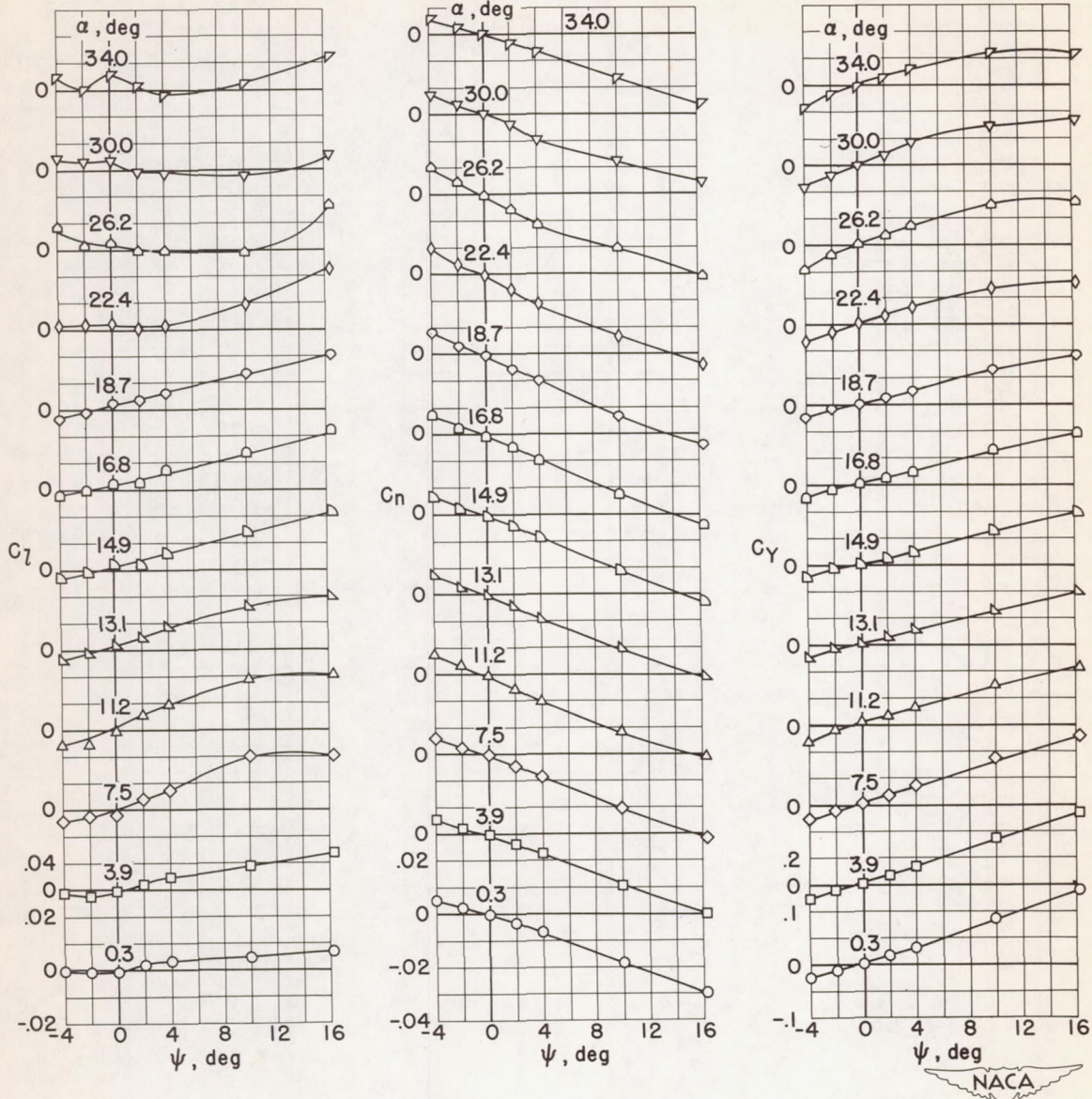
(a) Position 75-1 (top portion only).

Figure 16.- The effects of fins and fin positioning on the variations of C_L , C_N , and C_Y with ψ . Configuration A; fin 2. $R \approx 6.0 \times 10^6$.



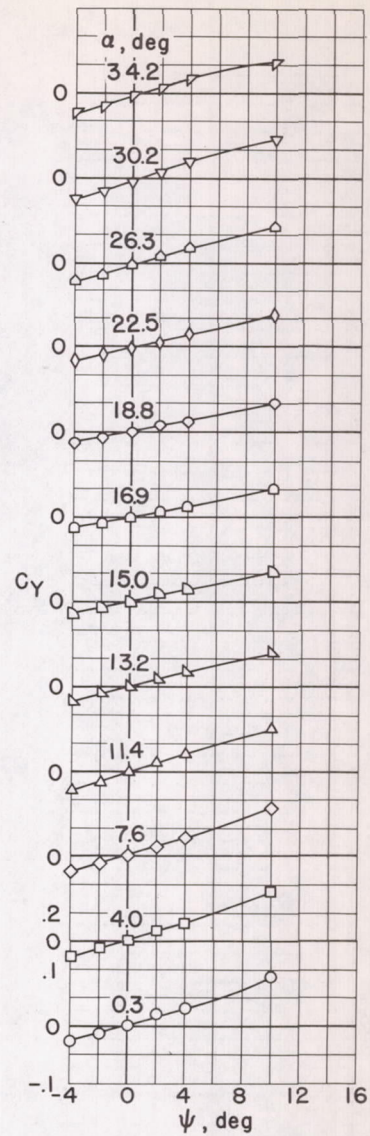
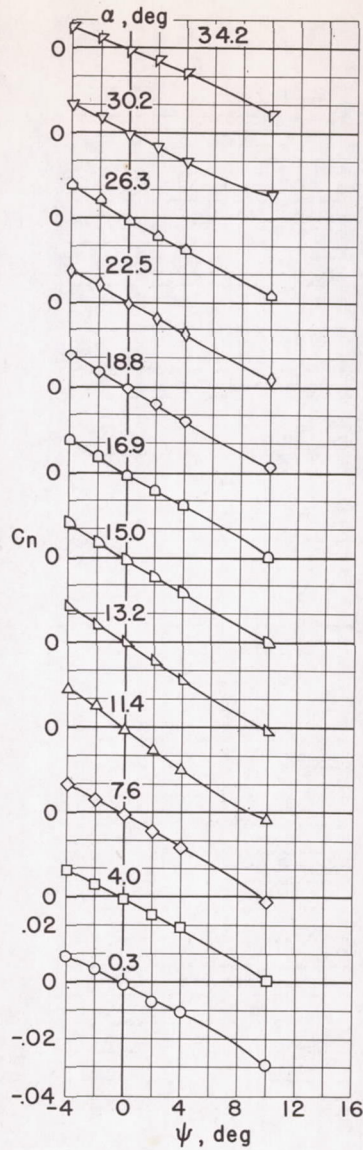
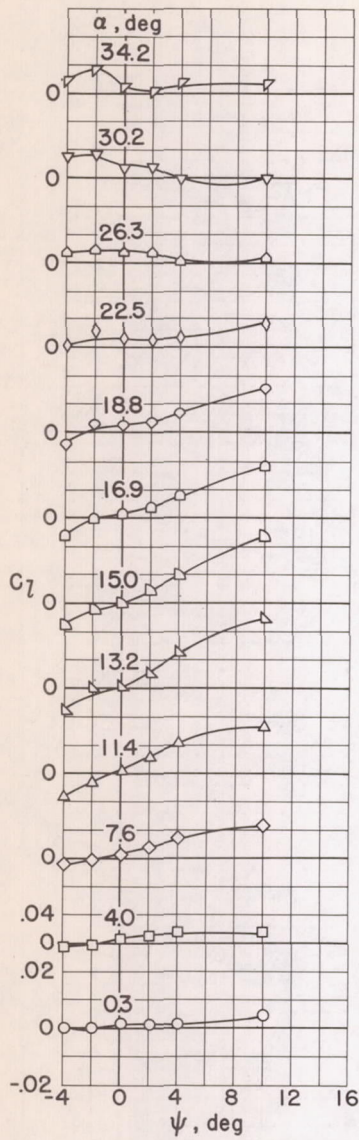
(b) Position 75-1.

Figure 16.- Continued.



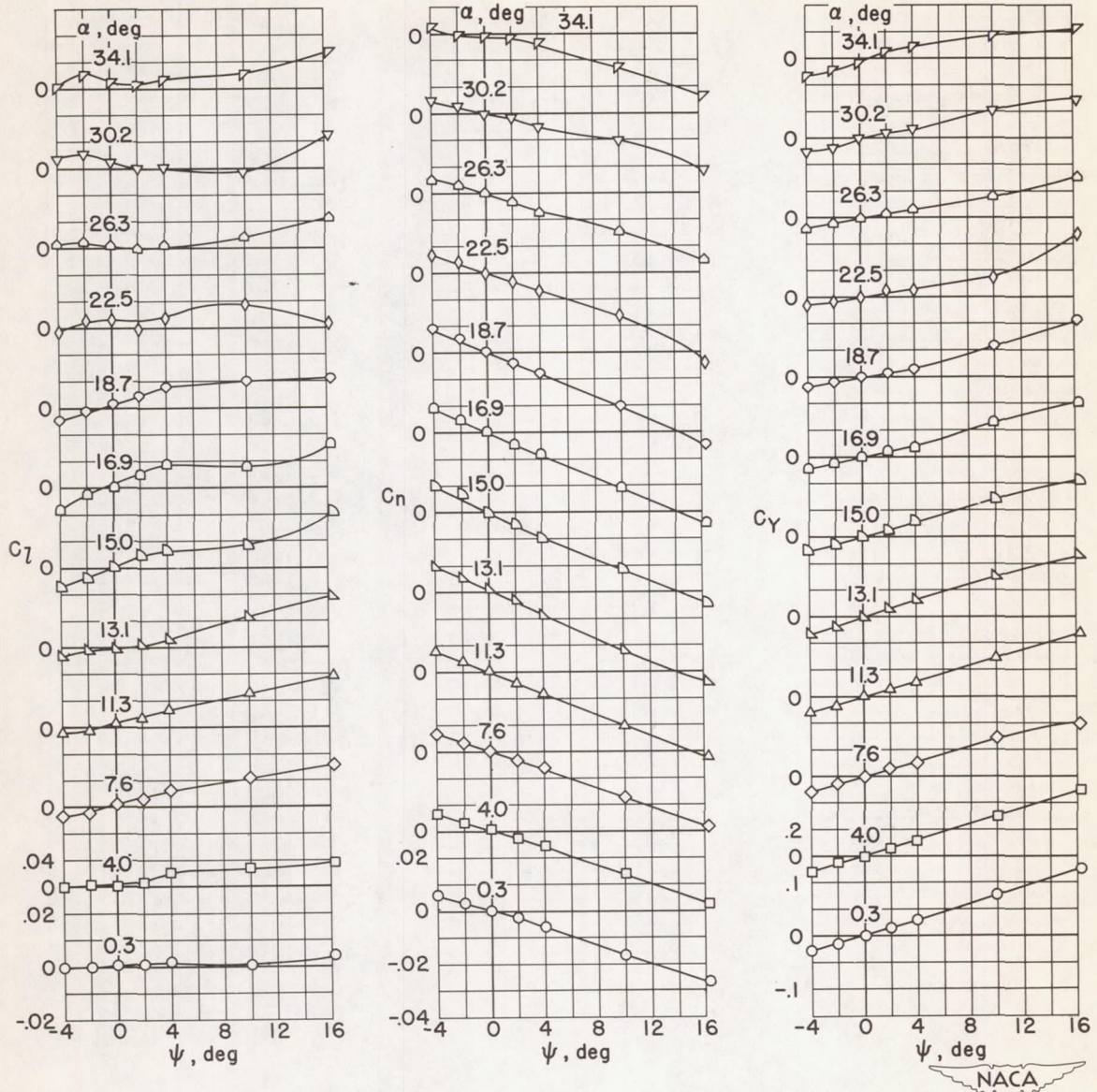
(c) Position 60-1.

Figure 16.- Continued.



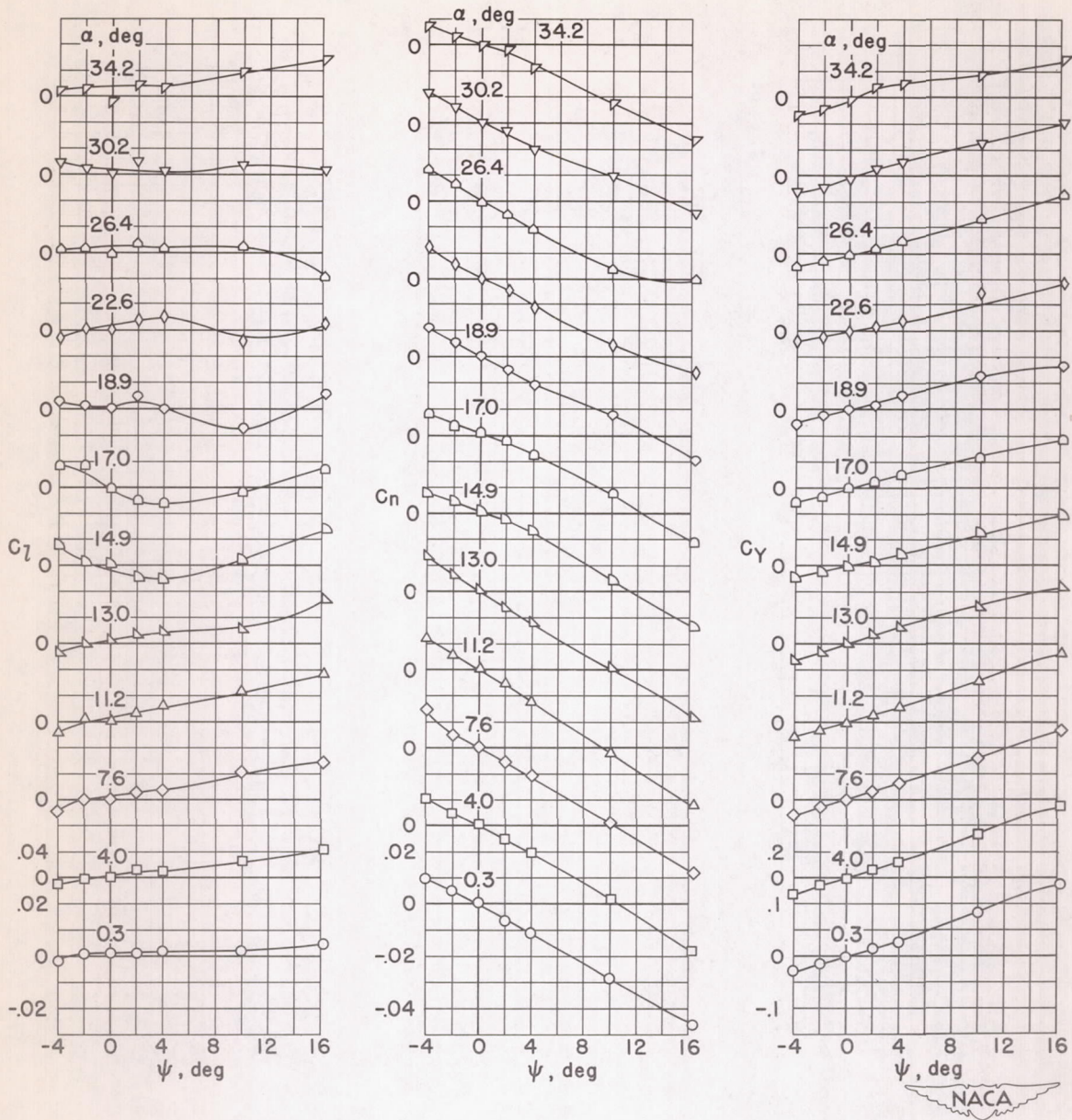
(d) Position 60-2.

Figure 16.- Continued.



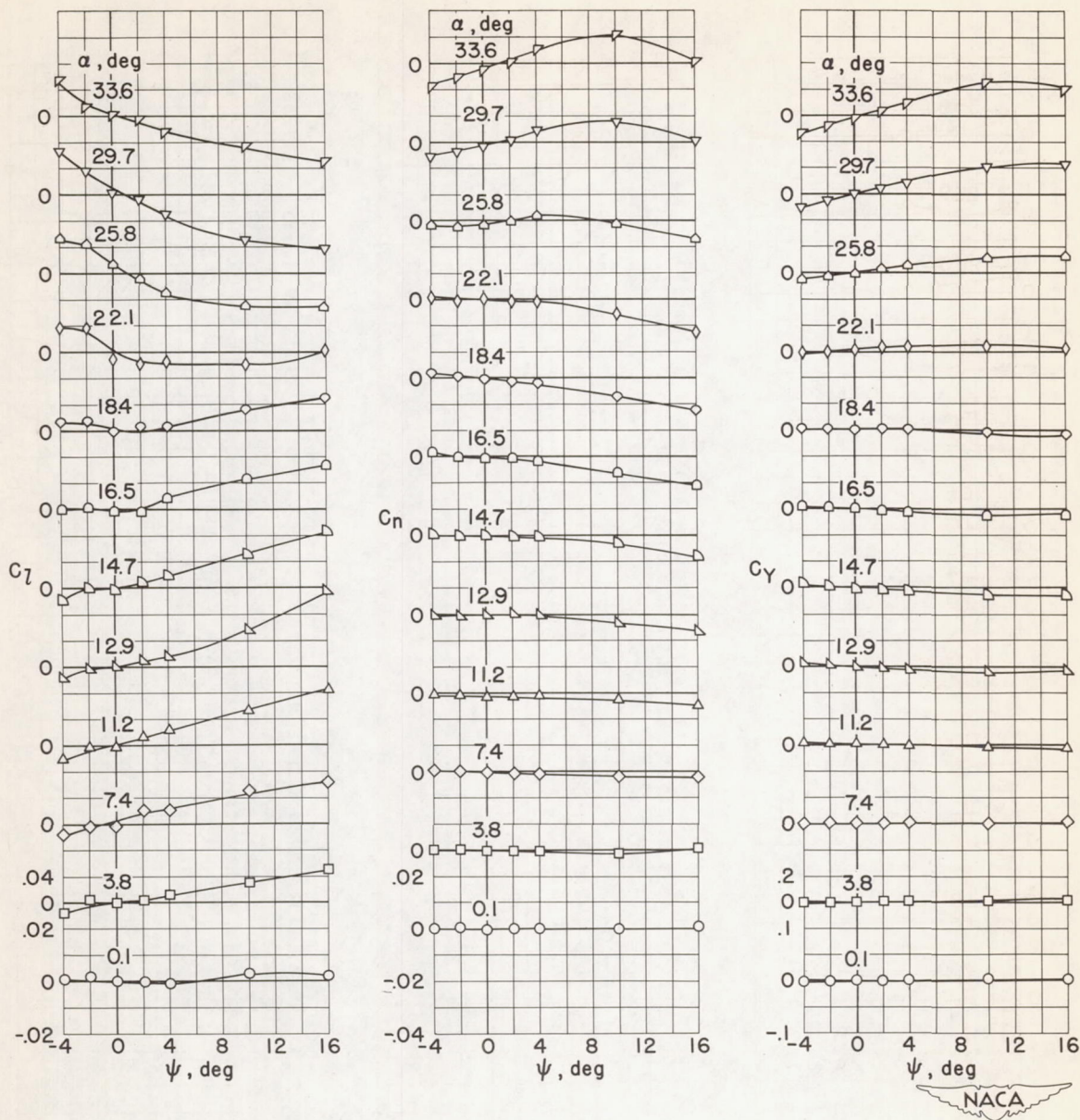
(e) Position 45-2.

Figure 16.- Continued.



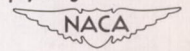
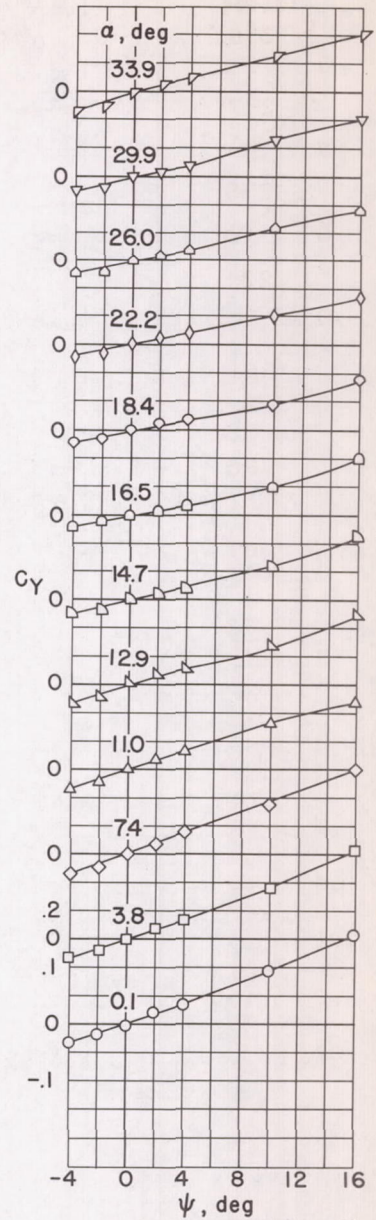
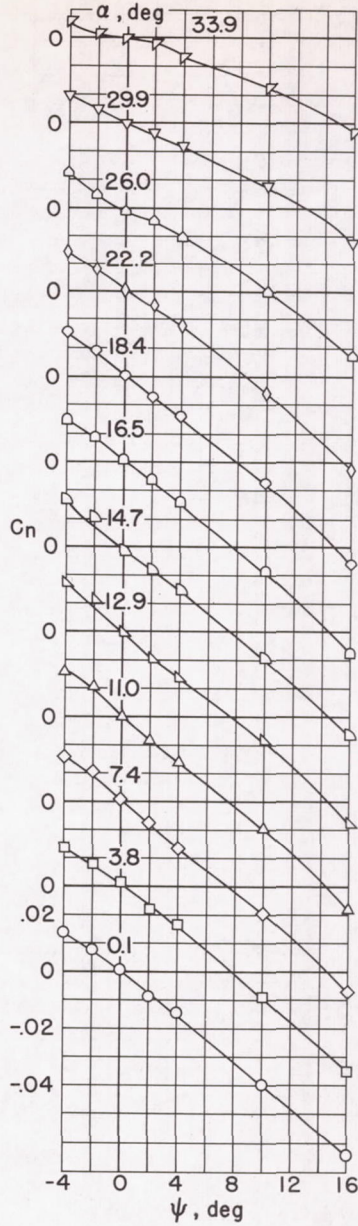
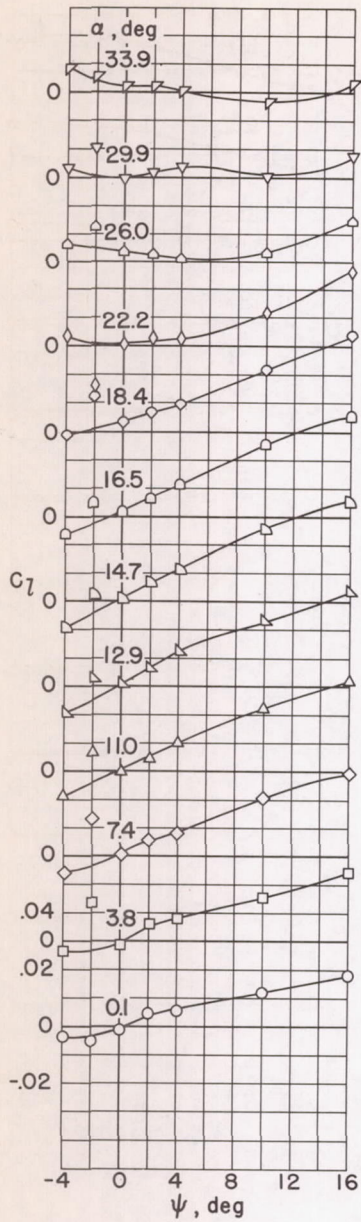
(f) Position 45-3.

Figure 16.- Concluded.



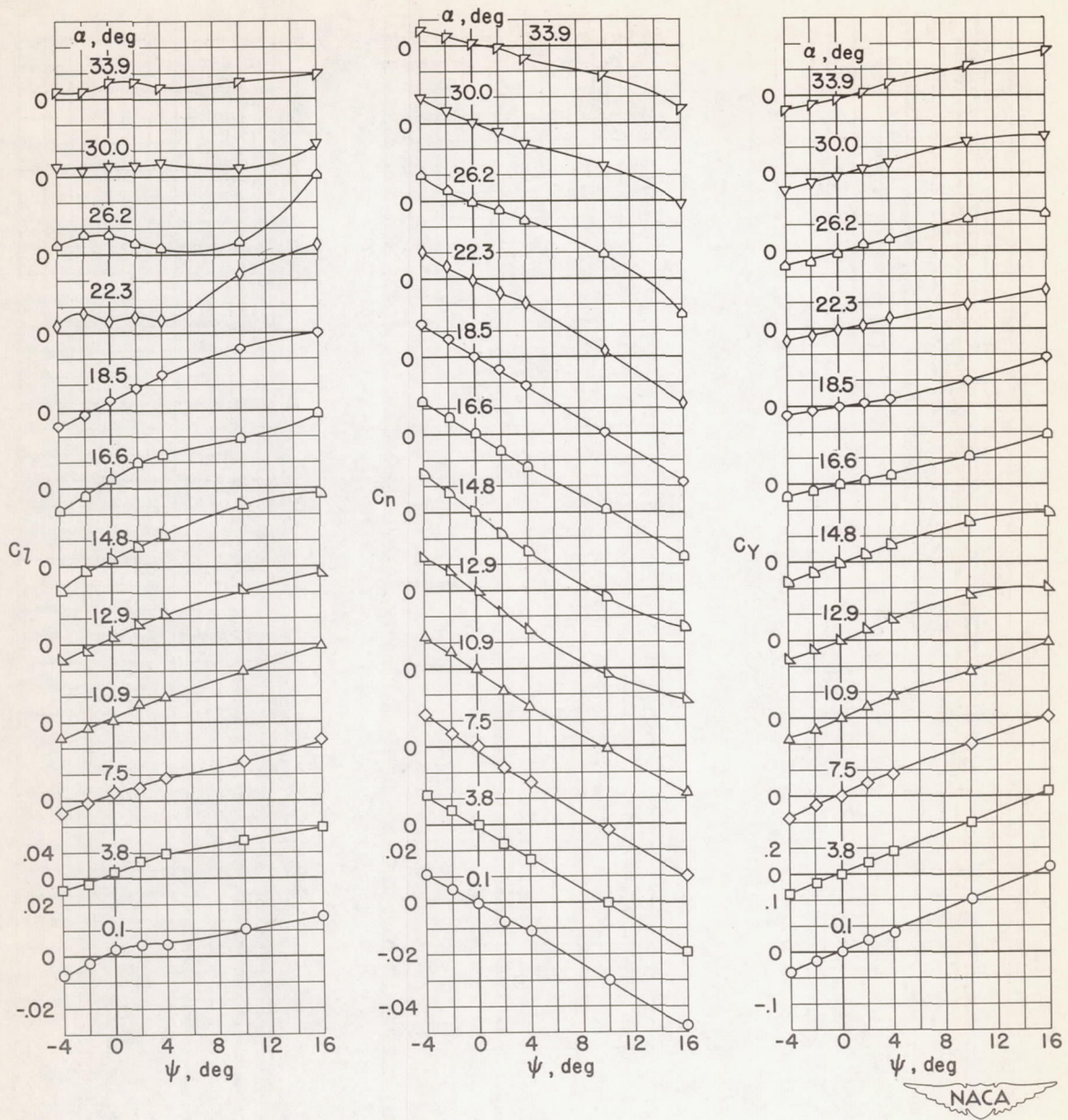
(a) Fins removed.

Figure 17.- Effect of fins and fin positioning on the variations of C_L , C_n , and C_Y with ψ . Configuration B, fin 1. $R \approx 6.0 \times 10^6$.



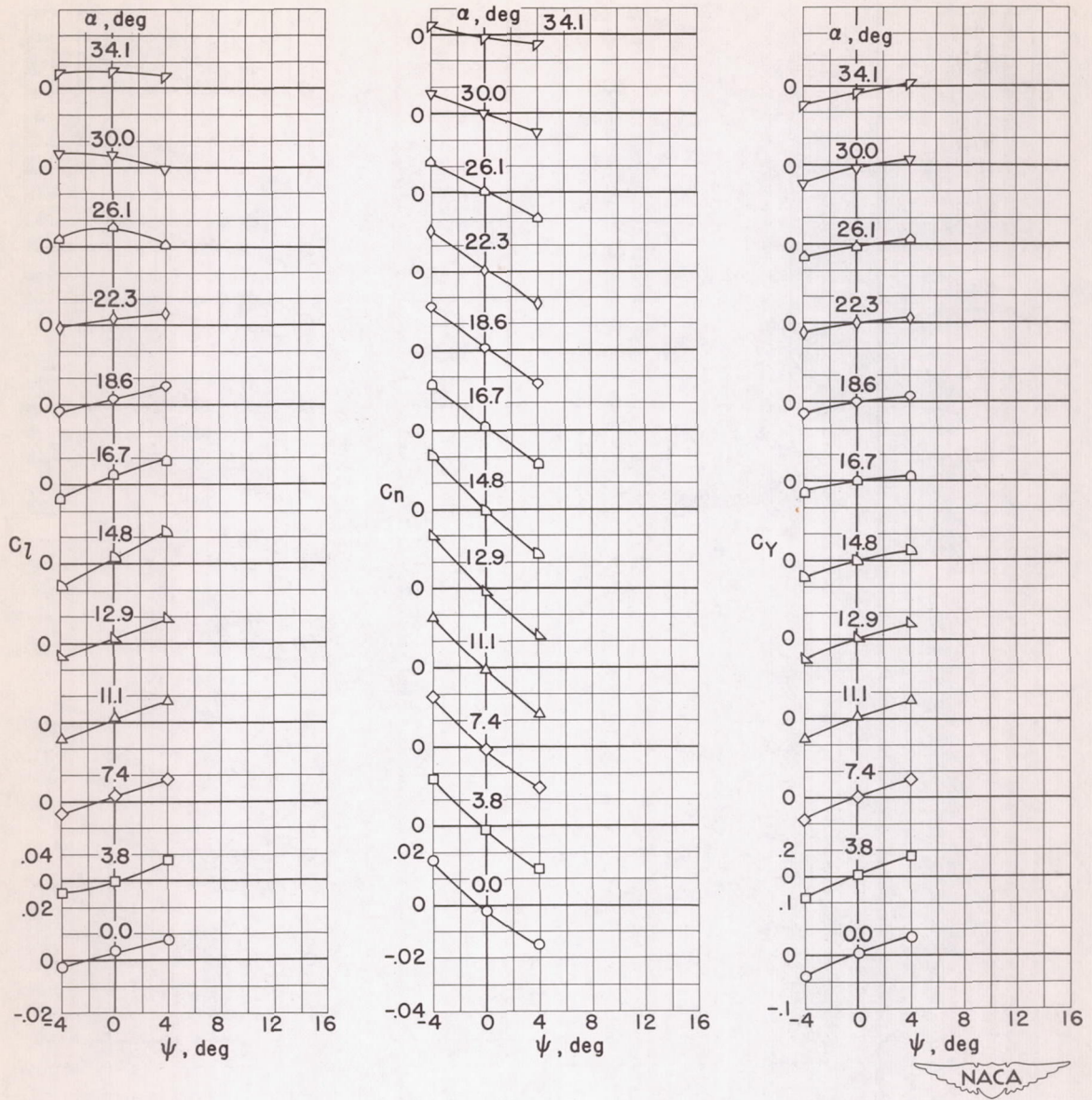
(b) Position 75-1.

Figure 17.- Continued.



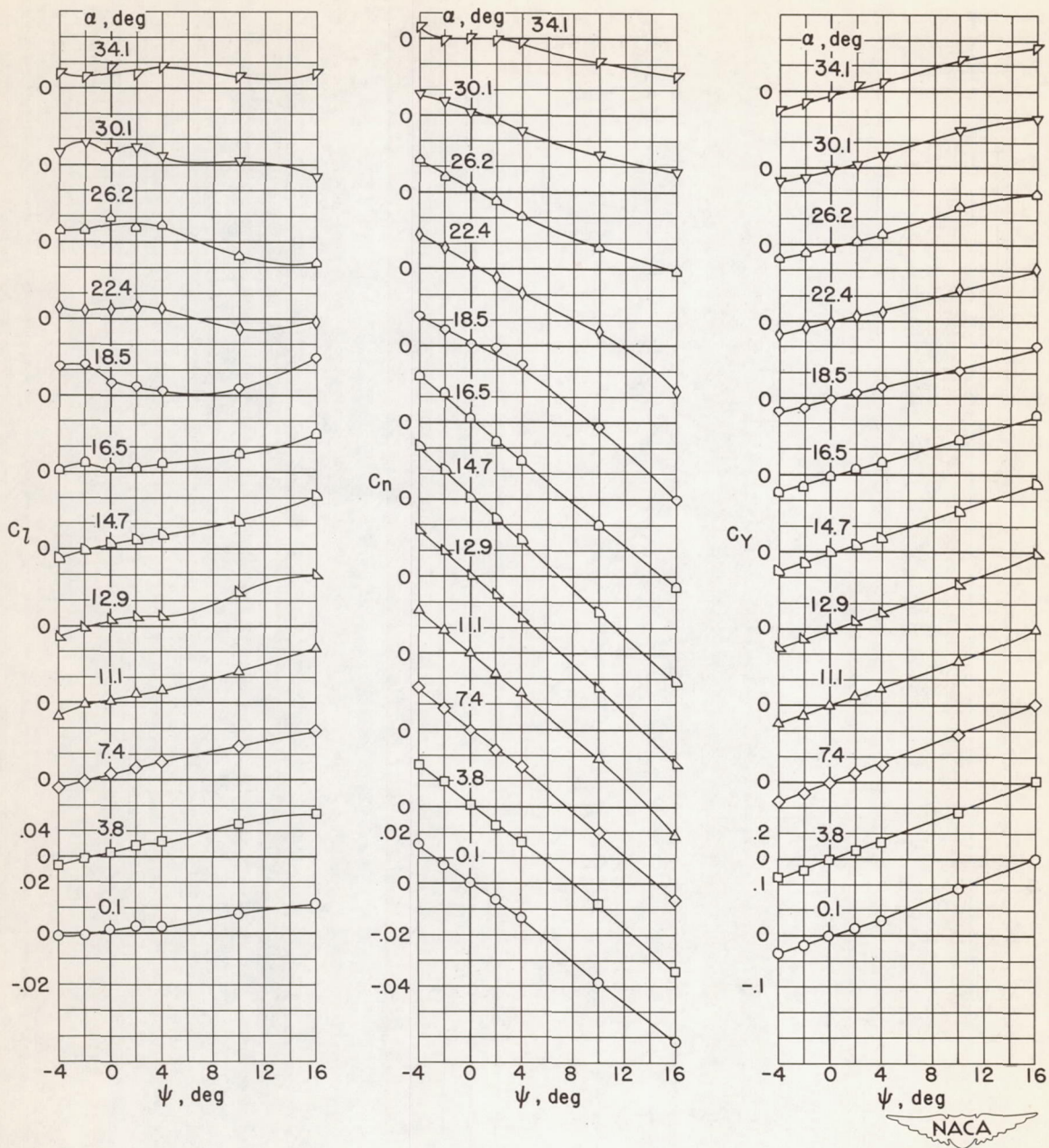
(c) Position 60-1.

Figure 17.- Continued.



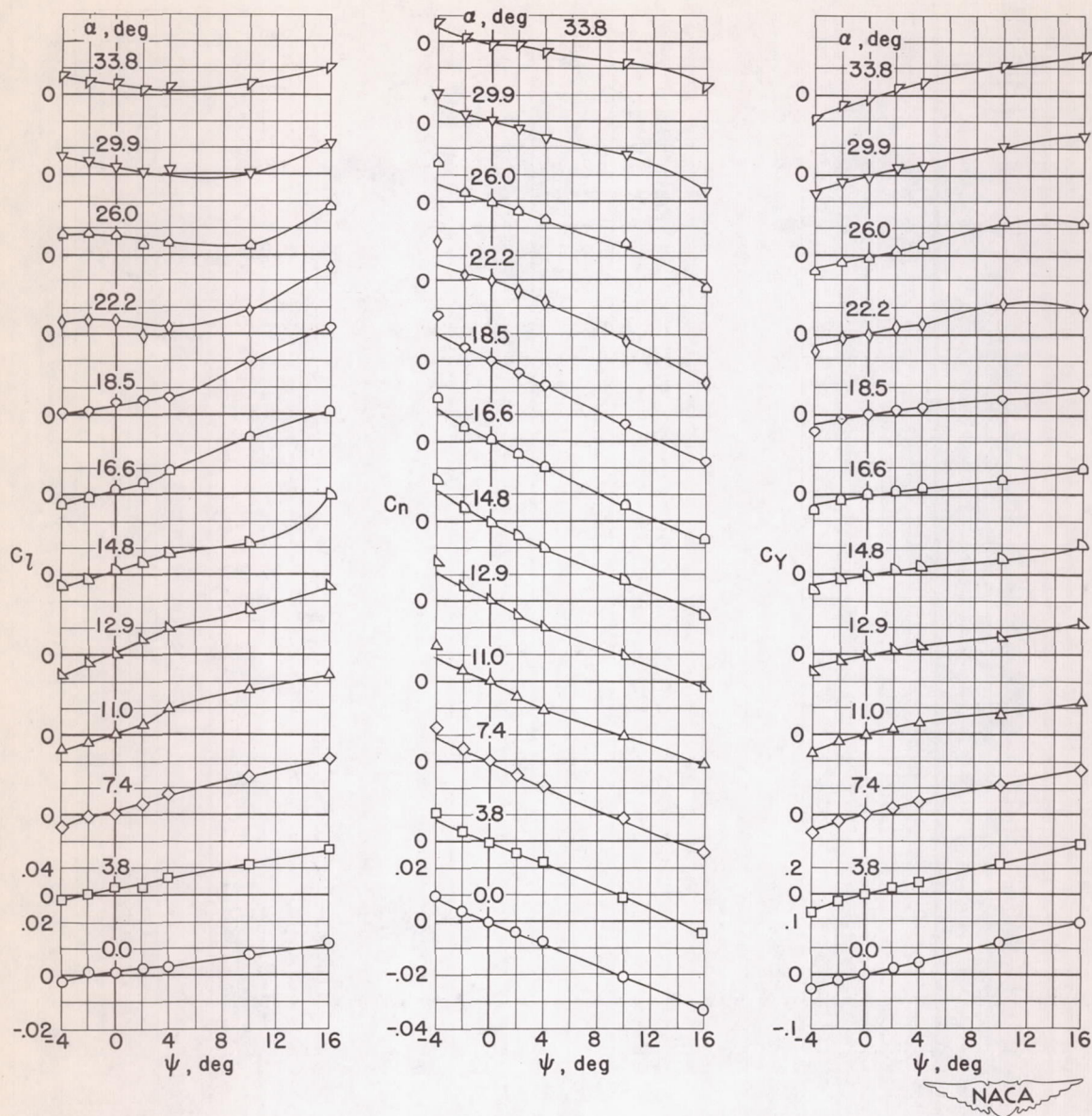
(d) Position 60-2.

Figure 17.- Continued.



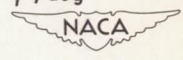
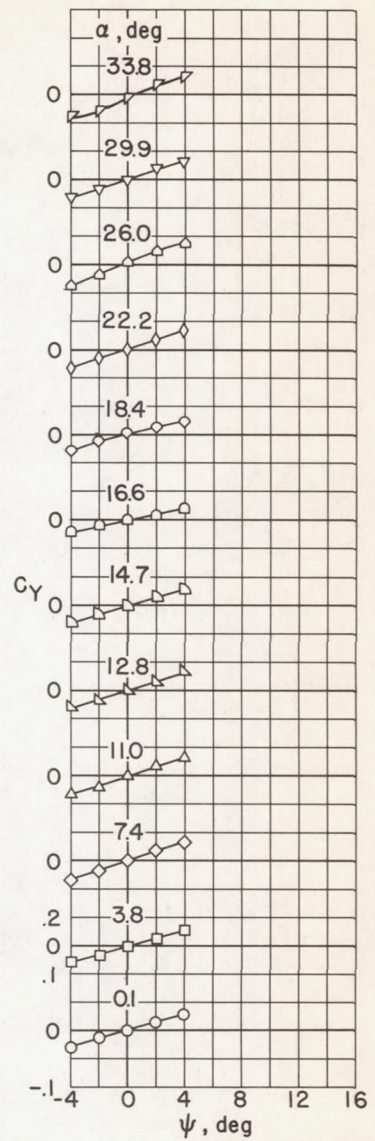
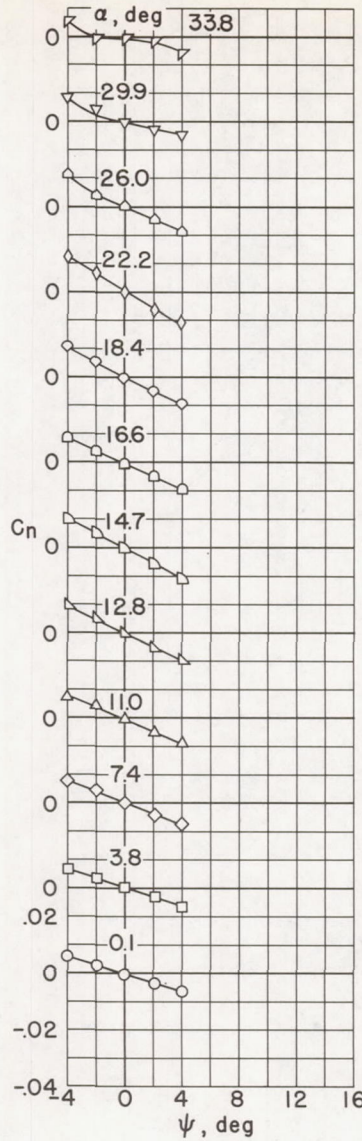
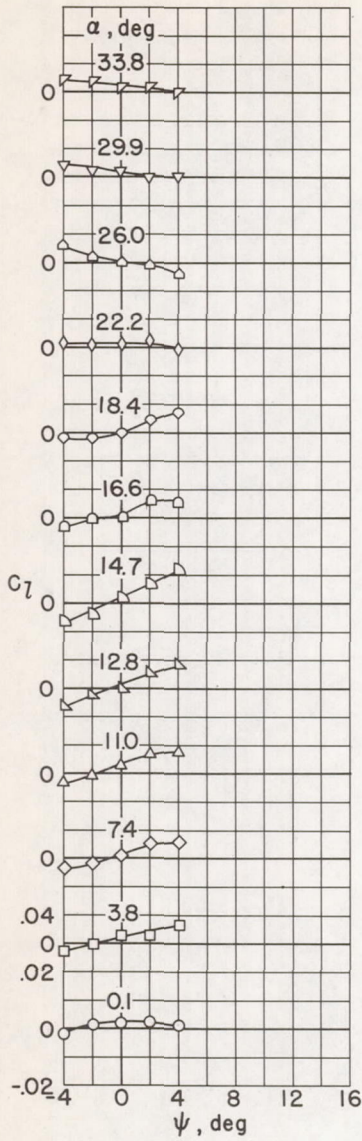
(e) Position 45-3.

Figure 17.- Concluded.



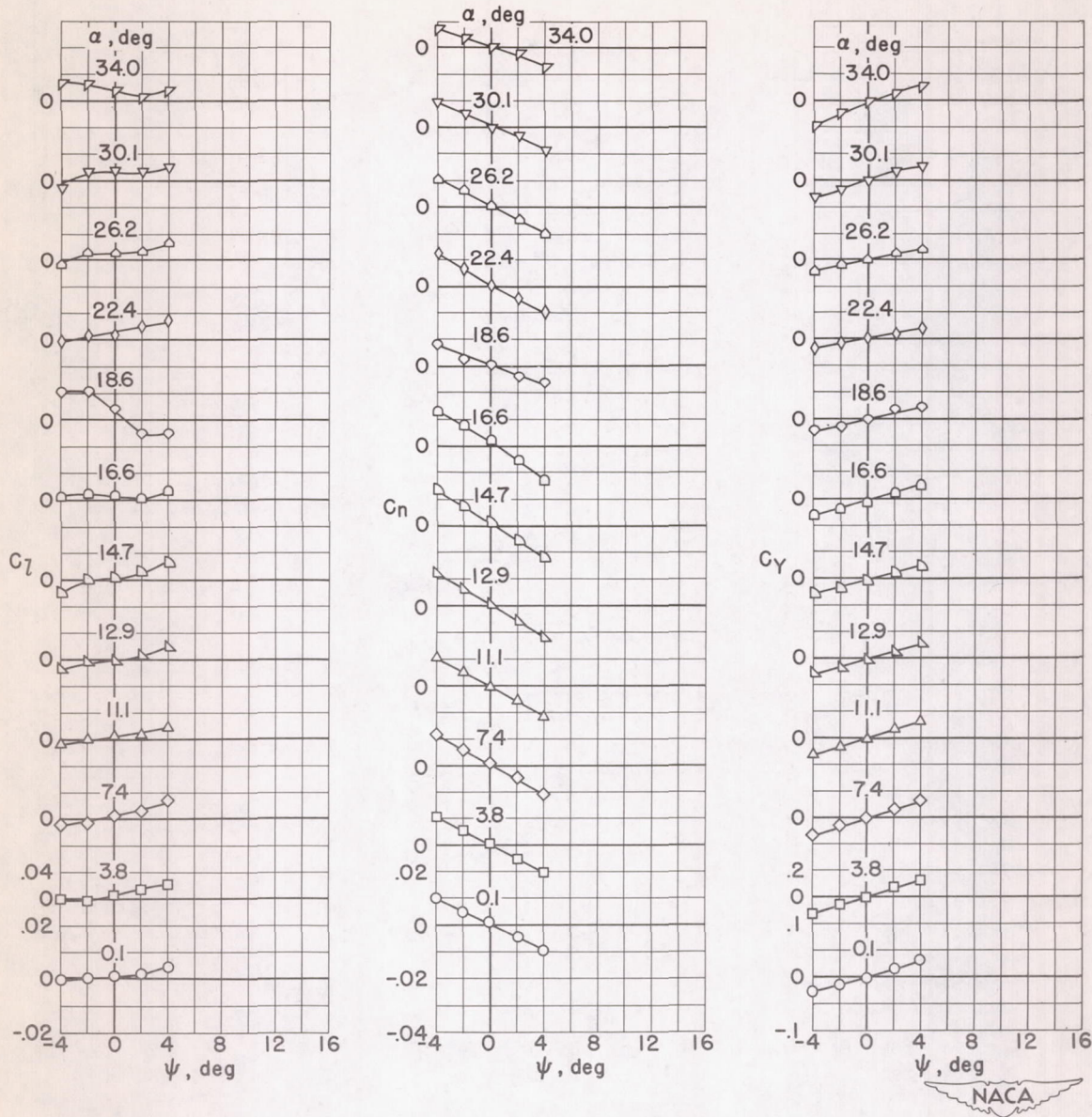
(a) Position 75-1.

Figure 18.- Effect of fins and fin positioning on the variations of C_l , C_n , and C_y with ψ . Configuration B; fin 2. $R \approx 6.0 \times 10^6$.

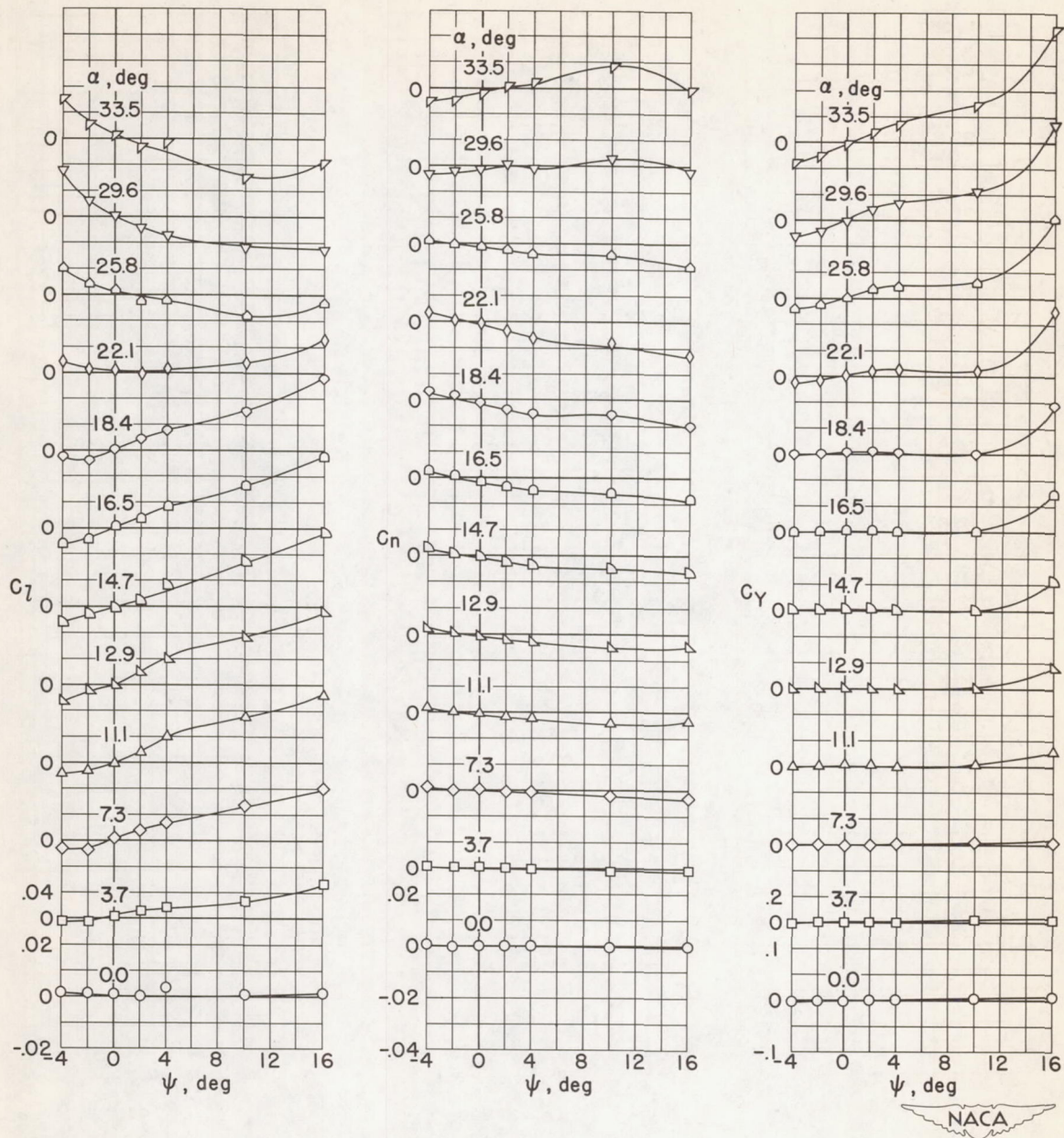


(b) Position 60-1.

Figure 18.- Continued.

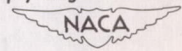
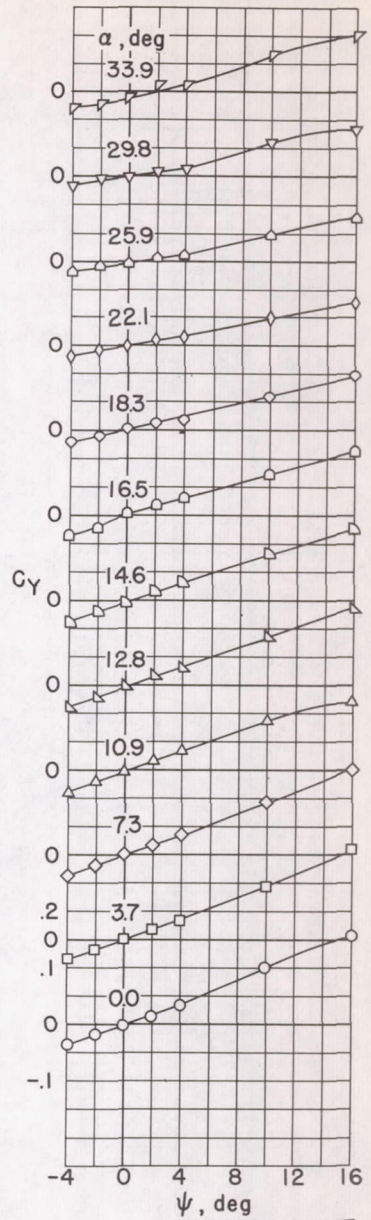
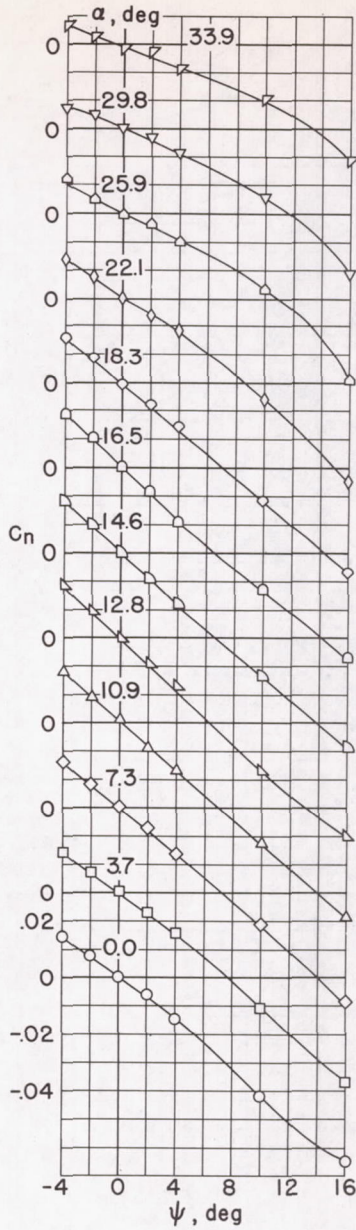
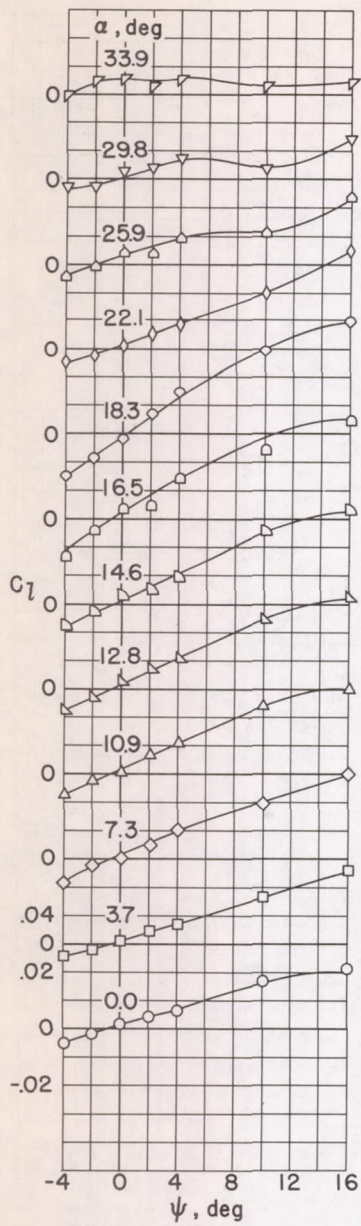


(c) Position 45-3.
 Figure 18.- Concluded.



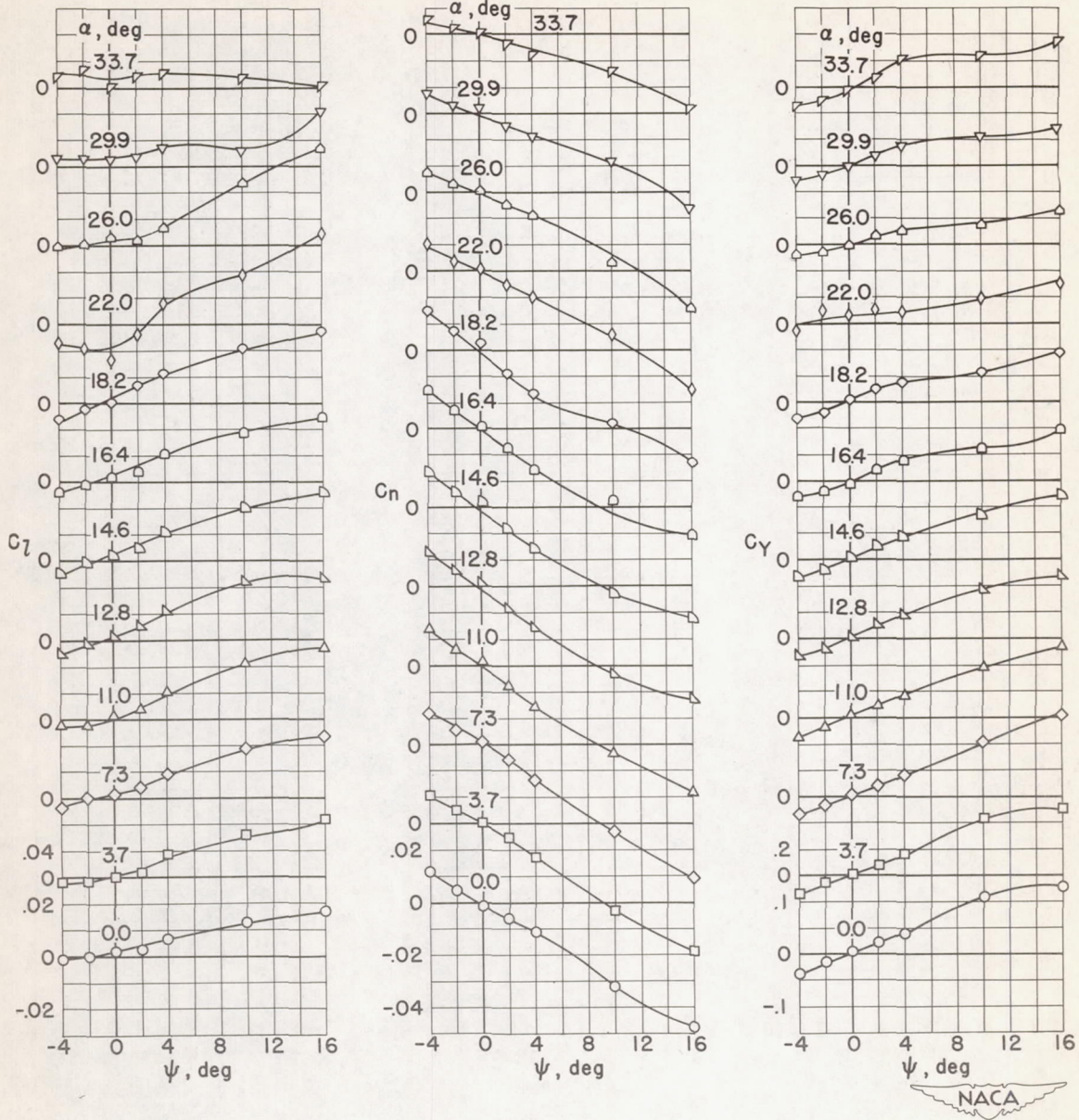
(a) Fins removed.

Figure 19.- Effect of fins and fin positioning on the variations of C_L , C_n , and C_Y with ψ . Configuration C; fin 1. $R \approx 6.0 \times 10^6$.



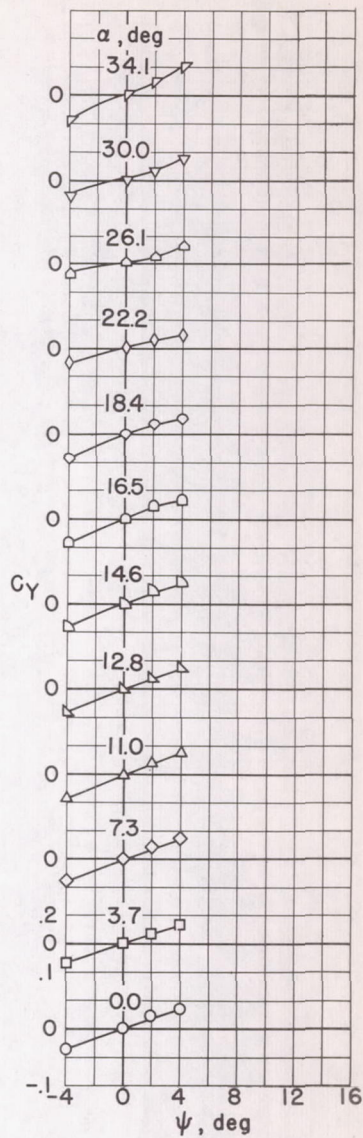
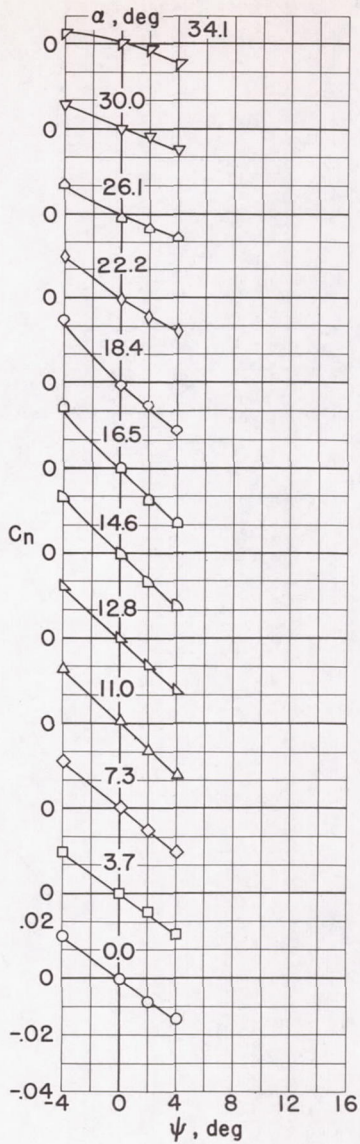
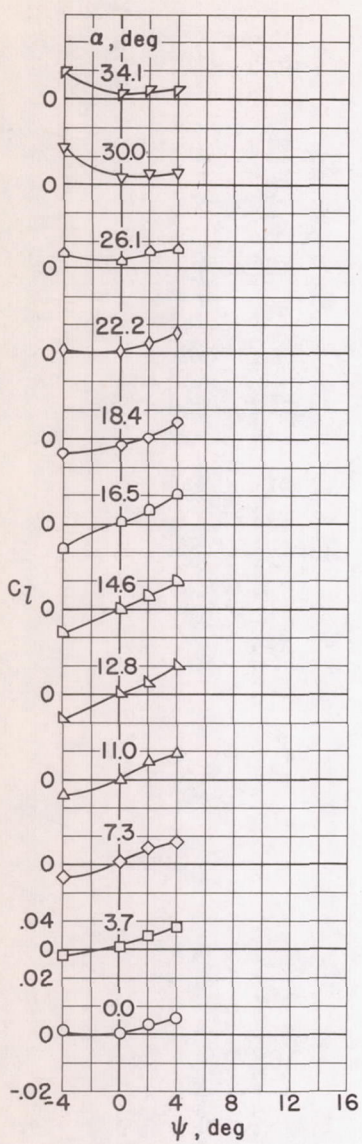
(b) Position 75-1.

Figure 19.- Continued.



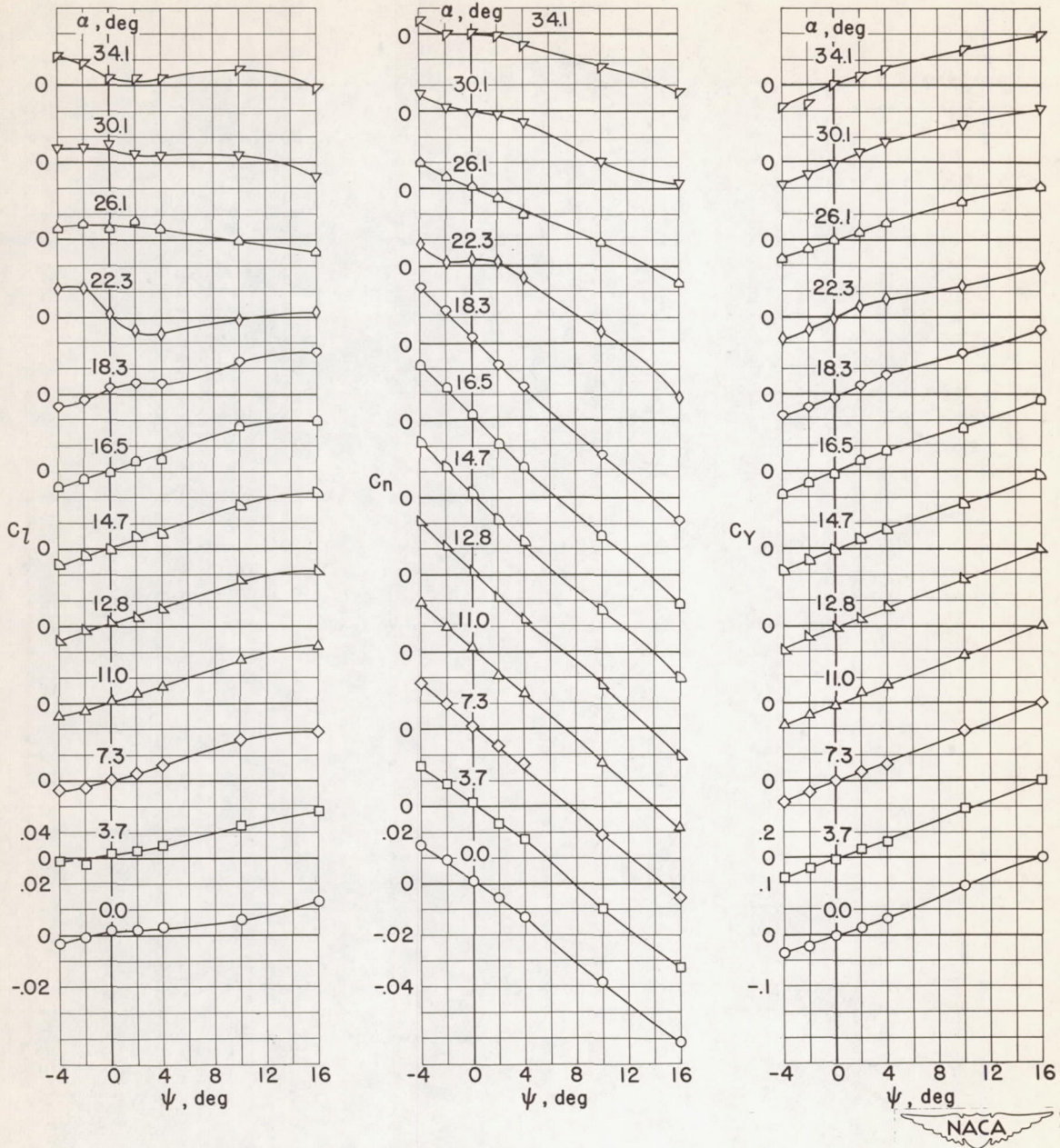
(c) Position 60-1.

Figure 19.- Continued.



(d) Position 60-2.

Figure 19.- Continued.



(e) Position 45-3.
Figure 19.- Concluded.